Chaos

Emergence, survival and segregation of competing gangs

H. Pérez-Martínez,[1,2,a)] F. J. Bauzá,[2,3] D. Soriano-Paños,[2,4] J.Gómez-Gardeñes,[1,2,5] and L. M. Floría[1,2,b)]
[1)]*Department of Condensed Matter Physics, University of Zaragoza, 50009 Zaragoza (Spain).*
[2)]*GOTHAM lab, Institute for Biocomputation and Physics of Complex Systems (BIFI), University of Zaragoza, 50018 Zaragoza (Spain).*
[3)]*Department of Theoretical Physics, University of Zaragoza, 50009 Zaragoza (Spain).*
[4)]*Institute Gulbenkian of Science (IGC), 2780-156 Oeiras (Portugal)*
[5)]*Center for Computational Social Science, University of Kobe, 657-8501 Kobe (Japan).*

(Dated: 11 May 2022)

In this paper we approach the phenomenon of criminal activity from an infectious perspective by using tailored compartmental agent-based models that include the social flavor of the mechanisms governing the evolution of crime in society. Specifically, we focus on addressing how the existence of competing gangs shapes the penetration of crime. The mean-field analysis of the model proves that the introduction of dynamical rules favoring the simultaneous survival of both gangs reduces the overall number of criminals across the population, as a result of the competition between them. The implementation of the model in networked populations with homogeneous contact patterns reveals that the evolution of crime substantially differs from that predicted by the mean-field equations. We prove that the system evolves towards a segregated configuration where, depending on the features of the underlying network, both gangs can form spatially separated clusters. In this scenario, we show that the beneficial effect of the coexistence of two gangs is hindered, resulting in a higher penetration of crime in the population.

Building on a recently introduced kinetic model[1,2] on the dynamics of norm violating (corrupt) behavior, we here analyze the effects of the competition between two criminal gangs in the spreading of asocial behaviors on a population. While the mean-field analysis reveals the benefits of adopting a selective punishment strategy, in which the majority gang is more harassed, in networked populations the gang competition leads to segregated configurations, rendering inefficient the strategy of selective punishment as both gangs do not compete locally.

The analysis of human behavior and its evolution in different periods and contexts has been one of the most relevant problems for different branches of science[3–5]. Sociology, economics, urban planning, and epidemiology are, among others, disciplines in which the understanding of human behavior and decision making play an essential role. For complex systems science, this problem has been tackled through the mathematical modeling of systems composed of a multitude of interacting elements in which the microscopic rules of interaction or imitation and the network of contacts between individuals capture, in a stylized way, different phenomena relevant to human dynamics[6]. Example of these approaches are models based on evolutionary game theory[7–9], models for the diffusion of cultural traits[10,11] and complex contagion models designed for the propagation of opinions[12–14] and the creation of polarized states[15]. In spite of the capacity of these models to explain qualitatively different aspects of human behavior, their practical interest has been, until recently, strongly limited by the lack of data that would make possible their experimental validation or allow their calibration to estimate the value of the parameters used in their formulation.

The advent of the Internet era, the increase in computing capacity and, more importantly, the possibility of obtaining individualized data of human activity with high spatio-temporal resolution through, for example, cell phone or wearable devices, have led to the development of a new approach to the study of human behavior usually termed as computational social science[16–19]. In this regard, computational social science has enabled to obtain an accurate cartography of human interactions[20–23], mobility patterns[24–26], socioeconomical inequalities[27,28] and to design large-scale experiments in which the imitation rules under different controlled conditions are tested[29–33].

The large amount of data capturing different aspects of human behavior and the possibility of their large-scale analysis have not detracted from the importance of studying models of human behavior[34,35]. On the contrary, in addition to making possible the validation of the hypotheses and the fine and precise calibration of current models, the advent of the big data era has been very beneficial for the theoretical side, pushing the frontiers of modelling towards new challenges where empirical evidence of the underlying microscopic mechanisms behind macroscopic phenomena is not yet available. It is in this area that modelling generates new knowledge beyond its direct application to concrete problems and systems.

Following this more theoretical facet of complex systems modelling, in this article we propose a compartmental framework, similar to those used in the study of epidemic models, which allows us to capture a series of essential ingredients in the propagation of crime. Such infectious-like perspective has been previously applied to the study of the spread of gunshot violence[36] and economic corruption[37–39]. Unlike other approaches based on evolutionary game theory [40–43], asocial behavior is not (explicitly) seen as a mechanism or strategy of profit for the corrupt agent, and its diffusion is not governed by the calculation of expected benefits. Inspired by previous works[1,2], here we conceptualize the criminal behavior as an infectious state associated with those agents violating

[a)]Electronic mail: h.perez@unizar.es
[b)]Electronic mail: mario.floria@gmail.com

a social norm or convention. In these references, a compartmental model is developed consisting of three states: Honesty (H), gathering the adopters of the social norm, Corruption (C), comprising those violating the norm, and Ostracism (O) , representing the punishment (the hallmark of norm violation[44,45]) to corrupt individuals, thus receiving the name of HCO model. The agents of the system are distributed among the compartments, and can transit from one to another by interacting with other agents following some imposed rules. In its simplest formulation, this gives rise to the following flows among compartments:

- Corruption flow: Agents H can be corrupted by interacting with their neighbors C, with a rate f_α dependent on a probability α:

$$H \xrightarrow{f_\alpha(C)} C\,. \tag{1}$$

- Delation flow: Agents C can be delated by interacting with their neighbors H, passing to ostracism at a rate f_β given by some probability β. It is this mechanism that differs from traditional approaches in the SIRS model by requiring the mediation of honest (healthy) individuals for the recovery of corrupt (infected) ones.

$$C \xrightarrow{f_\beta(H)} O\,. \tag{2}$$

- Reinsertion flow: O agents reintegrate into the honest population at a certain rate r, without requiring interaction with their neighbors.

$$O \xrightarrow{r} H\,. \tag{3}$$

The reinsertion rate is constant and independent of the environment, while the corruption f_α and delation f_β rates depend on microscopic processes in the agent's neighborhood, and thus are functions of the state of neighboring agents. It follows that the rate f_α (resp. f_β) must be null in the absence of agents C (resp. H) in the neighborhood. The original publication[1] further considers an additional flow ("warning to wrongdoers" effect) that allows corrupt agents to return to the H state without going through O, so including the possibility for a C agent to change his behavior for fear of being punished.

The HCO model allows us to preserve the social flavor of the mechanisms governing the evolution of crime while overcoming some of the limitations posed by traditional approaches relying on evolutionary game theory, such as the choice for the rules to update population's strategies[46]. Likewise, although later we restrict our analysis to the impact of pairwise interactions, the general formulation of both the corruption and delation rates as arbitrary functions, f_α and f_β respectively, allows for accommodating more complex contagion processes, such as those requiring higher-order interactions[6,12,47].

In reference[1] the authors analyzed in full detail the mean-field approximation to the dynamics of the HCO model, and its comparison with the numerical results of Monte Carlo (MC) simulations on random and non-random regular networks, for a type of simple one-variable *contact interaction* functions f_α and f_β. The three-dimensional phase diagram of the model shows the existence of three generic absorbing states, namely (i) full honesty, (ii) full corruption and (iii) a mixed state with non-zero flow through all the flow channels. The model shows no multistability, and two continuous transitions "full honesty - mixed state" (corruption transition) and "full corruption - mixed state" (honesty transition), as the model parameters are tuned. However, the introduction[2] of the effects of social intimidation in the delation of corrupt people changes the nature of the smooth honesty transition into a discontinuous one, and the phase diagram shows regions in parameter space where both a fully honest population and a fully corrupt one can coexist as stable asymptotic solutions (bistability).

Building on this HCO model, we propose a framework to explore what happens when two different, conflicting, and excluding gangs are present in the same population. Gang competition is widespread and usually results in violence, either intended to increase social prestige[48] or to obtain economic resources[49]. Space plays a crucial role in the occurence and spread of gang violence[50–53], which we intend to characterize by applying our model to networks with different structural features.

We denote by C_{in} and C_{st} the two criminals' species, or gangs, and consider that their competition materializes by delating each other, i.e. a C_{st} agent can be delated by a C_{in} neighbor:

$$C_{st} \xrightarrow{f_\beta(H,C_{in})} O\,; \tag{4}$$

in a similar way, a C_{in} agent can be delated by a C_{st} neighbor

$$C_{in} \xrightarrow{f_\beta(H,C_{st})} O\,. \tag{5}$$

Note that, when an interaction between a C_{in} and a C_{st} agents takes place, both can be delated by their counterpart at the same time becoming O. These cross-delation events do not necessarily involve snitching, but could also represent inter-gang violence which could remove the victim from the network or lead to the arrest of an agent involved in the interaction. For simplicity, we consider all these possible outcomes inside the ostracism compartment, in analogy with the removed compartment in the traditional SIRS model.

Both species follow the same rules concerning their interaction (the aforementioned corruption and delation flows) with the honest species. Moreover, the agents in the ostracism follow the same rules as in the HCO model, and reinsert into the honest population at the same rate r, irrespective of the species they belonged to before their delation and the species that delated them. These rules define a new compartmental scheme, hereinafter denoted by HCCO model, whose flow diagram is shown in Figure 1. For simplicity, we do not include here neither the "warning to wrongdoers" nor the social intimidation effects.

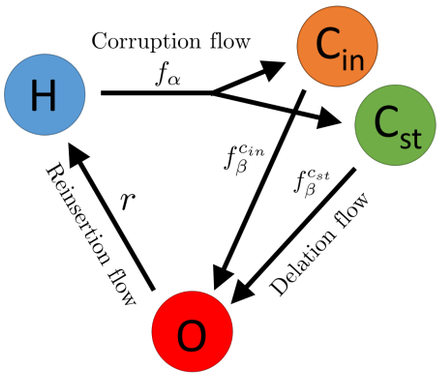

FIG. 1: Compartmental scheme and flows of the HCCO model.

The paper is organized as follows. Section I introduces the microscopic processes governing the stochastic evolution of the HCCO model and its conceptualization in form of a system of coupled Markov equations. Section II is devoted to the analysis of the results obtained from Monte Carlo (MC) simulations of the model and the numerical iteration of Markov equations. There, we show that the choice for the delation mechanism from the honest population to their criminal counterparts has a great impact on the equilibrium of the dynamics, ranging from a dominance regime where one gang prevales over the other one, which eventually disappears, to a configuration in which both gangs coexist. In the latter scenario, the discrepancies found between both results and the mean-field predictions reveal the crucial role played by the underlying network structure in shaping the competition between gangs. Specifically, we show that these discrepancies are explained by the segregation of the two gangs induced by the interplay between the dynamics and the structure of the connections, which becomes more relevant in presence of spatially correlated populations.

I. GANG COMPETITION: HCCO MODEL

The system is composed of N agents with pairwise interactions formally represented by an unweighted and undirected network defined by its adjacency matrix $\mathbf{A}$. At time step t the state of the agent i ($1 \leq i \leq N$), denoted by $\sigma_i(t)$, takes on values on the set $\{H, C_{in}, C_{st}, O\}$ of mutually exclusive states. From the assumptions that define the model in the introductory section, the stochastic (MC) simulations of the dynamics are implemented in the following way:

At each time step (t) for each agent i, whose state is $\sigma_i(t)$:

(*i*) If $\sigma_i(t) = O$, then $\sigma_i(t+1) = H$ with probability r, remaining O (out of society) with probability $1-r$.

(*ii*) If $\sigma_i(t) = C_{in}$, then $\sigma_i(t+1) = O$ with transition probability $f_\beta^{in}(i, \{\sigma_j\})$, a (yet unspecified) function of the local configuration around i. Thus, agent i keeps belonging to her gang at $t+1$ with probability $(1 - f_\beta^{in})$.

(*iii*) If $\sigma_i(t) = C_{st}$, then $\sigma_i(t+1) = O$ with transition probability $f_\beta^{st}(i, \{\sigma_j\})$, a (yet unspecified also) function of the local network configuration around i. The agent remains in her gang with probability $(1 - f_\beta^{st})$.

(*iv*) If $\sigma_i(t) = H$, then the agent can become corrupt with probability $f_\alpha(i, \{\sigma_j\})$ (to be specified later), remaining honest with probability $(1 - f_\alpha)$. Given that both gangs are mutually exclusive, we must introduce a function $g(x,y)$ denoting the probability of enrolling the gang x in presence of the gang y. Then, if $N_{c_{in}}(i)$ and $N_{c_{st}}(i)$ denote the number of C_{in} and C_{st} neighbors of i, we have:

(a) $\sigma_i(t+1) = C_{in}$ with probability $f_\alpha(i, \{\sigma_j\}) \times g(N_{c_{in}}(i), N_{c_{st}}(i))$;

(b) $\sigma_i(t+1) = C_{st}$ with probability $f_\alpha(i, \{\sigma_j\}) \times g(N_{c_{st}}(i), N_{c_{in}}(i))$.

In what follows, we assume a proportionality rule so that $g(x,y) = \frac{x}{x+y}$ and $g(x,y) + g(y,x) = 1$.

Our choice for the transition probabilities mimics the familiar implementation of infectious processes in MC simulations of epidemiologic models with pairwise interactions. Therefore, as in the corruption flow in the original HCO model, we account for a probability α, with $\alpha \in [0,1]$, that a honest agent becomes criminal for each contact with any criminal counterpart. Then after interaction of the H agent with all its neighbors, the transition probability to crime is

$$f_\alpha(i, \{\sigma_j\}) = 1 - \prod_{j=1}^{N} (1 - \alpha A_{ij} (\delta_{\sigma_j, C_{in}} + \delta_{\sigma_j, C_{st}})), \quad (6)$$

and the agent is enrolled in a gang proportionally to the fraction of the gangsters in its neighborhood (as indicated by the function g above).

A criminal C_{in} (respectively C_{st}) can be delated by a C_{st} (resp. C_{in}) neighbor with probability β, with $\beta \in [0,1]$. Besides, it can be delated by a H neighbor with a probability β^{in} (resp. β^{st}). To avoid the inconvenience of a model with too many parameters, the simplest choice is to assume that $\beta^{in} = \beta^{st} = \beta$, i.e. honest agents do not discriminate between gangs, and they delate both kind of gangsters with equal probability (and equal to the inter-gang delation probability). In the Appendix, where the mean-field approximation to the dynamics is analyzed in some detail, we prove that for this choice (non-selective delation) the two gangs cannot coexist asymptotically. The minority gang in the initial conditions becomes asymptotically extinct, and the behavior of the model is that of the HCO model. This is due to the hampered corruption power and the higher exposure to delation events of the minority gang, which becomes even less populated as time goes by, until extinction. This mean-field result also holds in MC simulations of the model. Therefore, it seems convenient to consider a situation in which the honest agents delate preferentially the majority gang. To implement this "selective delation", while keeping the number of parameters at its minimum, we introduce a function of the fractions $\langle C_{in} \rangle$ and $\langle C_{st} \rangle$,

say $B(\langle C_{in}\rangle,\langle C_{st}\rangle)$, defined as

$$B(x,y)=\begin{cases}1 & \text{if } x\geq y\,,\\ \exp\left[-\frac{1}{T}\frac{(y-x)}{(x+y)}\right] & \text{if } x<y\,,\end{cases} \tag{7}$$

and assume $\beta^{in}=B(\langle C_{in}\rangle,\langle C_{st}\rangle)\times\beta$, and $\beta^{st}=B(\langle C_{st}\rangle,\langle C_{in}\rangle)\times\beta$. Note that the parameter T, non negative, in the function B controls the (exponential in gang size difference) decay of the delation of the minority gang by honest agents. We recover the non-selective delation case by simply taking $B(x,y)=1$.

After interaction with all its neighbors, we write the probability that a C_{in} agent becomes an O agent as

$$f_\beta^{in}(i,\{\sigma_j\})=1-\prod_{j=1}^{N}\left[1-\beta A_{ij}\left(\delta_{\sigma_j,C_{st}}+B(\langle C_{in}\rangle,\langle C_{st}\rangle)\delta_{\sigma_j,H}\right)\right]. \tag{8}$$

In an analogous way, the probability that a C_{st} agent is delated reads

$$f_\beta^{st}(i,\{\sigma_j\})=1-\prod_{j=1}^{N}\left[1-\beta A_{ij}\left(\delta_{\sigma_j,C_{in}}+B(\langle C_{st}\rangle,\langle C_{in}\rangle)\delta_{\sigma_j,H}\right)\right]. \tag{9}$$

One can associate to this MC dynamics a non-linear Markov process, following references[54], by assigning to each agent i, at each time t, a real vector $\vec{\rho}(i;t)$ of components:

$$\vec{\rho}(i;t)=(\rho_h(i;t),\rho_{c_{in}}(i;t),\rho_{c_{st}}(i;t),\rho_o(i;t)) \tag{10}$$

where $\rho_x(i;t)$ represents the probability of belonging to the compartment x. The time evolution of the probabilities of agent i is determined by the interactions with its neighbors, and is easily described by a matrix $\mathbf{Q}$ such that $\vec{\rho}(i,t+1)=\mathbf{Q}\vec{\rho}(i,t)$, where

$$\mathbf{Q}=\begin{pmatrix}1-f_\alpha & 0 & 0 & r\\ f_\alpha g(\rho_{c_{in}}^T(i),\rho_{c_{st}}^T(i)) & 1-f_\beta^{in} & 0 & 0\\ f_\alpha g(\rho_{c_{st}}^T(i),\rho_{c_{in}}^T(i)) & 0 & 1-f_\beta^{st} & 0\\ 0 & f_\beta^{in} & f_\beta^{st} & 1-r\end{pmatrix}, \tag{11}$$

where $\rho_{c_x}^T(i)=k^{-1}\sum_{j=1}^{N}A_{ij}\rho_{c_x}(j)$ is the total fraction of the species C_x in the neighborhood of agent i, and $g(x,y)=\frac{x}{x+y}$, as above. The corruption rate f_α is now

$$f_\alpha(i,\{\vec{\rho}(j)\})=1-\prod_{j=1}^{N}\left[1-\alpha A_{ij}\left(\rho_{c_{in}}(j)+\rho_{c_{st}}(j)\right)\right]. \tag{12}$$

The delation rates are now given by

$$\begin{aligned}f_\beta^{in}(i,\{\vec{\rho}(j)\})&=1-\prod_{j=1}^{N}\left[1-\beta A_{ij}\left(\rho_{c_{st}}(j)+B(\rho_{c_{in}}^T,\rho_{c_{st}}^T)\rho_h(j)\right)\right],\\ f_\beta^{st}(i,\{\vec{\rho}(j)\})&=1-\prod_{j=1}^{N}\left[1-\beta A_{ij}\left(\rho_{c_{in}}(j)+B(\rho_{c_{st}}^T,\rho_{c_{in}}^T)\rho_h(j)\right)\right],\end{aligned} \tag{13}$$

where $\rho_{c_x}^T=N^{-1}\sum_{i=1}^{N}\rho_{c_x}(i)$ $(x=in,st)$ represents the total fraction of the species C_x in the system.

In the Appendix we prove, in the case of selective delation, that the mean-field approximation predicts that the coexistence of both gangs is generic. Moreover, it turns out that in the state of coexistence of competing gangs, the fraction of honest agents is significantly higher than in the single-gang state. This is easily realized from the consideration that the mutual delation of competing gangs decreases the total fraction of criminals. In a scenario of strongly competing gangs, one might say that, perhaps counterintuive as it may seem at first sight, a clever strategy for the decrease of corruption is to tolerate the minority gang to allow its agents to do the "dirty work" of contributing to the delation of the stronger gang. The mean-field analysis in the Appendix provides a supportive argument of this somewhat machiavellian, unscrupulous, point of view.

To check the predictions of the mean-field approximation, we will compare them with the results of the Markov dynamics and MC simulations on random and non-random networks. We restrict our attention to networks with a fixed degree k, which are expected to be closer to the mean-field assumptions than those with degree heterogeneities. The first choice is a random regular network (RRN) where pairs of nodes are randomly linked, while strictly keeping the same degree k for all the nodes, so the system has no spatial structure. We use RRN networks of degree $k=4$ with $N=10^4$ nodes. We also use a square planar lattice of the same size $N=10^4$ and periodic boundary conditions. Due to its spatial structure, one should expect the results on the lattice to be more different from the mean-field predictions than those on a RRN.

II. RESULTS

Unless otherwise stated, all results on networks have been obtained as an average of 100 system realizations for each value of the model parameters, starting with a population nearly equally divided between the honest state and both gangs, $(\rho_h,\rho_{c_{in}},\rho_{c_{st}})_{t=0}=(0.4,0.3,0.3)$. In the case of Markov simulations, initial probabilities for each agent are randomly assigned (i.e. non-homogeneous initial conditions), with the constraint that the sum of probabilities for all agents match this condition. In Figures 2a-b we show some examples of the honest population fractions obtained for the Markov dynamics and MC simulations on RRN. One can note the good fit between the mean-field predictions and the results obtained with the Markov dynamics, although some appreciable deviations occur for certain ranges of the parameters α and β. In particular, when the honest population fractions are relatively small, the Markov dynamics departs from mean-field behavior, being closer to the behavior exhibited by the system under Monte Carlo simulations. This effect becomes more pronounced the smaller the total honest fraction. A deviation of this kind in the Markov dynamics is an indication that the network structure on which we implement the model has a clear and non-negligible influence on the dynamics of the system, which the mean-field is unable to capture. The fact that these

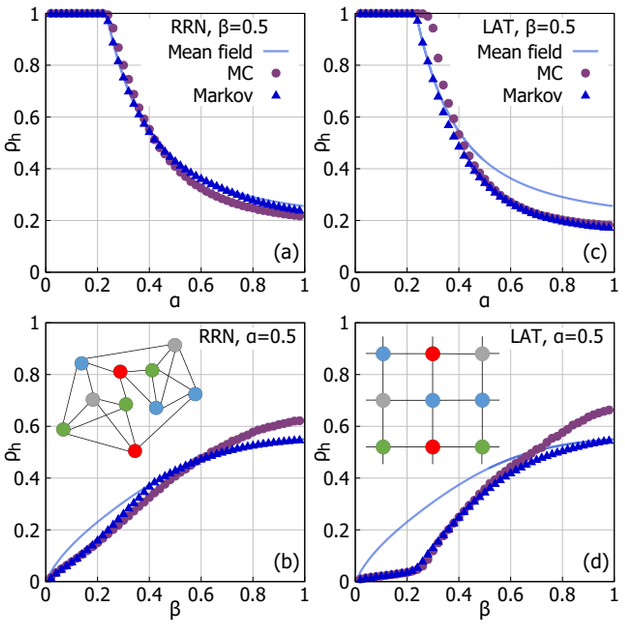

FIG. 2: Fraction of honest population in equilibrium in the case of gang coexistence, for $r = 0.5$, $k = 4$. Results are shown for RRN as a function of α (a) and β (b), and for the lattice as a function of α (c) and β (d). All the networks used have 10^4 nodes. We compare the mean-field, Markov and Monte Carlo (agent based) simulations. The results are averaged over 100 different realizations for every value of α and β, with initial conditions $(\rho_h, \rho_{c_{in}}, \rho_{c_{st}}) = (0.4, 0.3, 0.3)$. For Markov simulations, initial fractions of the species on each node are random, although giving rise to the same global fraction of species.

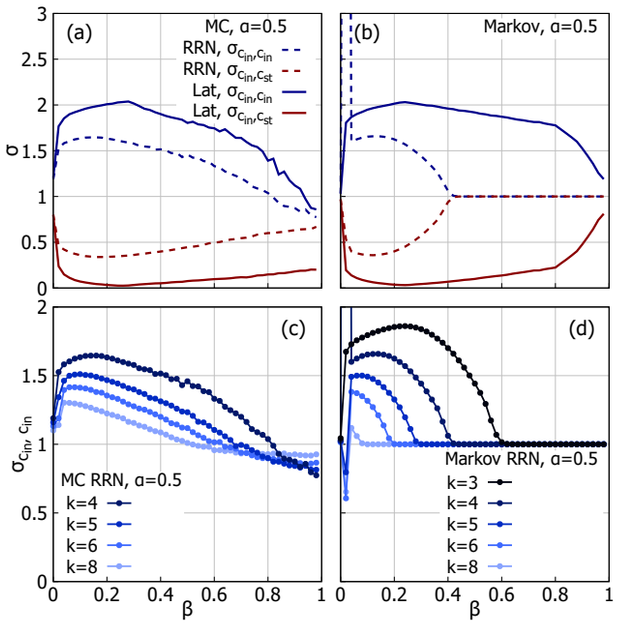

FIG. 3: Measures of segregation between gangs. Results are shown as a function of β for $\alpha = 0.5$. Top panels: Measures of the intra-gang (dark blue) and inter-gang (dark red) segregation, for Monte Carlo (a) and Markov (b) simulations, and for RRN (solid lines) and lattice (dashed lines). Bottom panels: Intra-gang segregation for Monte Carlo (c) and Markov (d) simulations, on RRN and for different values of nodes degree k.

deviations coincide almost perfectly with the behavior of the Monte Carlo simulations in some areas indicates that the underlying mechanism giving rise to the deviations is common to both. We also note that no differences are observed between mean-field and Markov dynamics for the single-gang HCO model, so that the deviations observed here have its origin in the gangs' competition.

In Figures 2c-d we show the corresponding results on the square planar lattice. We see that the almost coincidence of Markov dynamics and MC results for low values of the honest fraction extends now for a larger interval of those. Also, for both, low and high values of the honest fraction, the differences between MC results and mean-field are further strengthened. Then, as expected, the spatial structure reinforces the deviations from mean-field already present in the RRN.

To gain insight into the mechanisms of interplay between the model dynamics and the network characteristics we must quantify the heterogeneity in the state composition of local neighborhoods, as explained in the following.

Measuring neighborhoods' heterogeneity. Segregation

To quantify the deviations from the mean-field predictions we define in the equilibrium the quantities $\sigma_{x,y}$ (where $x, y \in \{H, C_{in}, C_{st}, O\}$) that measure how much, on average, the fraction of agents y in the neighborhoods of agents x deviates from that of a homogeneously distributed population. To be specific, for the system configurations of MC simulations in a homogeneous network of degree k, this measure is defined as the ratio of the number of interactions l_{xy} between species x and y to the number of interactions that should exist in a well-mixed population, $N_x \times k \times \rho_y^T$, where ρ_y^T is the total fraction of y agents in the population, and N_x is the total number of x agents:

$$\sigma_{xy}^{\mathrm{MC}} = \frac{l_{xy}}{N_x k \rho_y^T} = \frac{N}{k}\frac{l_{xy}}{N_x N_y} = \sigma_{yx}^{\mathrm{MC}}\,, \tag{14}$$

where we have used that $\rho_y^T = N_y/N$. If the value of $\sigma_{x,y}$ is less than 1, this means that species x has, on average, a smaller number of neighbors of species y than it should, and we will say that both species are segregated. Conversely, if it is greater than 1, the neighborhoods of x agents will be composed of more y agents than would correspond on average, and we say that both species are aggregated. Note that we can measure the degree of segregation between agents of the same species by setting $x = y$.

For the case of Markov configurations, where each agent i has probability $\rho_x(i)$ of belonging to species x, we define the number of interactions between x and y as the weighted sum of all existing interactions $l_{xy}^{\mathrm{MK}} \equiv \sum_{i,j=1}^{N} A_{ij}\rho_x(i)\rho_y(j)$, and divide it by the total weighted number of interactions

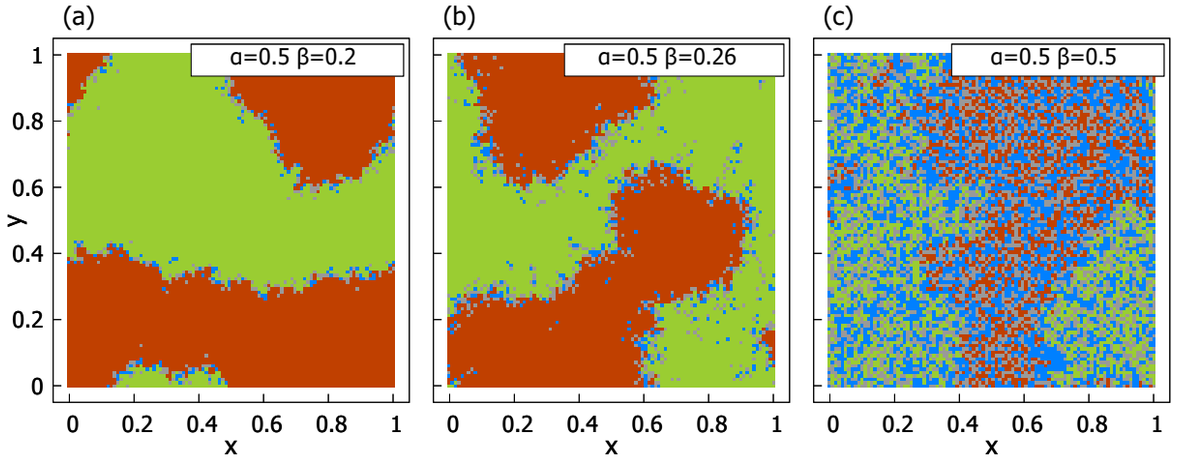

FIG. 4: Lattice configurations corresponding to single snapshots of Monte Carlo simulations of the HCCO model in equilibrium. Each square corresponds to a single agent, and its color determine the species she belongs to: honest (blue), C_{in} gang (green), C_{st} gang (orange) and ostracism (grey). Configurations correspond to values of β above, below and equal to β_c, namely $\alpha = 0.5$ and $\beta = 0.2 < \beta_c$ (a), $\beta = \beta_c = 0.26$ (b) and $\beta = 0.5 > \beta_c$ (c). β_c indicates the value in which penetration of honest agents inside corrupt aggregates takes place.

that there should be in a well-mixed population, $\sum_{i=1}^{N} \rho_x^i k \rho_y^T = \rho_x^T \times \rho_y^T \times k \times N$. Thus, the definition of $\sigma_{x,y}^{\mathrm{MK}}$ is

$$\sigma_{xy}^{\mathrm{MK}} = \frac{1}{Nk\rho_x^T\rho_y^T} \sum_{i,j=1}^{N} A_{ij}\rho_x(i)\rho_y(j) = \sigma_{yx}^{\mathrm{MK}} . \qquad (15)$$

We focus on the measures of segregation between gangs, $\sigma_{c_{in},c_{in}}$ and $\sigma_{c_{in},c_{st}}$, to reveal the effects of including two competing species in the model. The results of the Markov and Monte Carlo dynamics, both in RRN and lattice, are shown in Figure 3. First, the results of MC simulations show a very sharp segregation between gangs, such that agents in one gang tend to be largely surrounded by agents of the same gang ($\sigma_{c_{in},c_{in}} > 1$), and are far removed from those of the opposite gang ($\sigma_{c_{in},c_{st}} < 1$). Moreover, this segregation is much more pronounced in lattices than in RRNs, highlighting the importance of spatial structure. This implies that the system dynamics on networked populations are such that corrupt gangs are segregated, giving rise to local environments quite different from the overall network composition. This fact provides the basis for a rationalization of the differences in the results observed and the mean-field predictions.

We have seen above that the Markov dynamics shows clear differences between the region of the parameter space (high honesty values), where the results coincide with mean-field predictions, and the region where they are closer to MC behavior (low honesty values). Initially, in homogeneous networks, one would expect the Markov dynamics to be such that the probabilities at each node in equilibrium are equal to those at the other nodes, and equal to the fractions in equilibrium predicted by mean-field, and therefore, σ_{xy} must be equal to 1. Indeed, this is what is observed in our model when using homogeneous initial conditions, and also in the high honesty region starting with non-homogeneous initial conditions. In contrast, when the behavior resembles that obtained by MC simulations, the descriptors clearly indicate the presence of inter-gang segregation. These results are much more pronounced in the case of lattice networks than in RRN, as was also the case for the MC simulations.

It is well known that, in general, the higher the degree of the networks, the more similar the behavior of dynamics on networks is to the mean-field behavior, because in a more interconnected network, the environments of the agents are more similar to each other. We have studied how segregation behaves by varying the degree. The results are also shown in Figure 3, where we can clearly observe that as degree increases, segregation decreases, even disappearing completely for high values of k.

Segregation on lattices

To help the arguments leading to a satisfactory explanation of our results on networks on the basis of the segregation of gangs, we visualize in Figure 4 three MC lattice configurations at equilibrium, for different values of α and β, which correspond to situations of coexistence between gangs. Figure 4c corresponds to a higher β value, and thus has a higher total fraction of honest agents. At a glance, the segregation phenomenon we have described can be seen by the presence of two large groups or aggregates distributed in different regions of the space corresponding to both gangs, and a border in between rich in honest agents and ostracism. In the case of $\beta = 0.2$ (Figure 4a), all the honest and agents in ostracism are located at or near the border, while in the case of $\beta = 0.5$ (Figure 4c), they are more or less homogeneously distributed throughout the network. This implies that there is a certain critical value β_c above which the honest agents are able to penetrate the gangs aggregates, and survive by themselves inside. This critical value corresponds to the peak of the susceptibil-

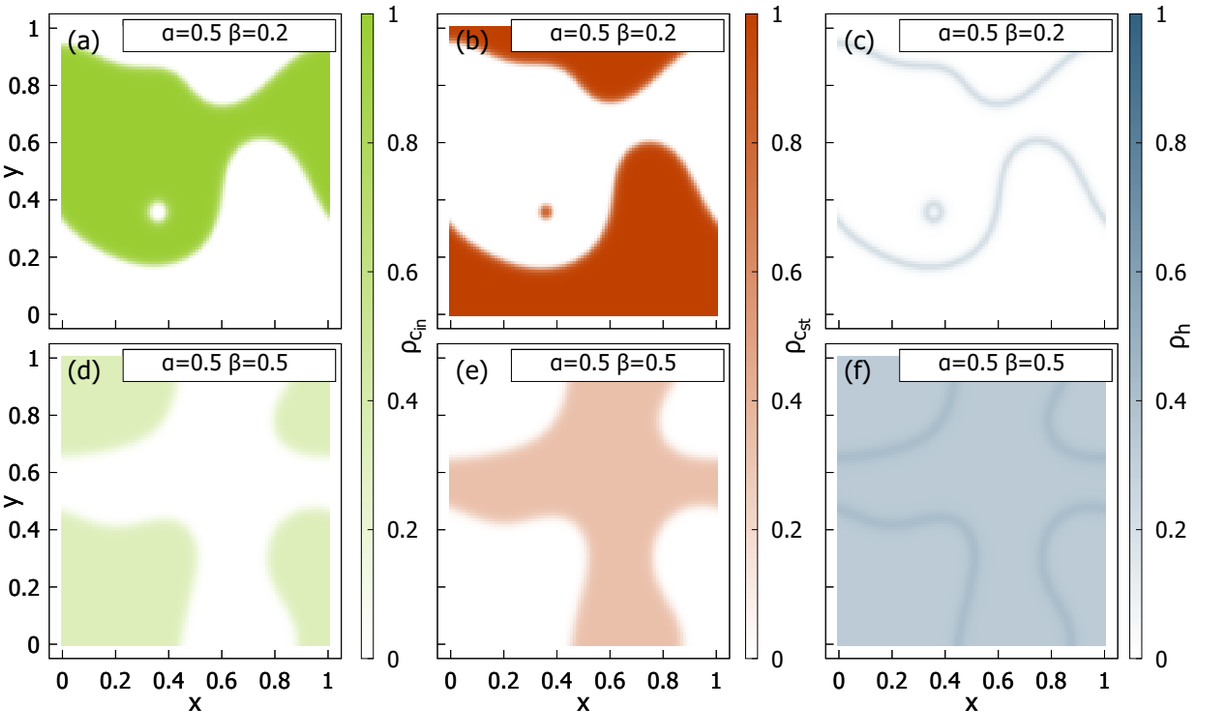

FIG. 5: Lattice configurations corresponding tosingle snapshots of Markov simulations of HCCO model in equilibrium. Each square corresponds to a single agent, and the color strength indicates the probabilities of each node belonging to each species: C_{in} (green) (a,d), C_{st} (orange) (b,e) and H (blue) (c,f). Configurations correspond to $\beta = 0.2 < \beta_c$ (a-c) and $\beta = 0.5 > \beta_c$ (d-f). Note that the lighter colors of the lower panels indicate lower penetration of corruption for higher β.

ity function estimated from several realizations of the HCO model on lattices, yielding $\beta_c = 0.26$. The associated HCCO configuration at this critical value is represented in Figure 4b.

A similar phenomenon occurs in the Markov case. We can see in Figure 5 that, for a choice of parameters where segregation occurs, two distinct criminal groups appear separated by a honest-rich frontier. Moreover, there is no coexistence between gangs within these aggregates, i.e., nodes within the aggregates contain only probabilities of belonging to one gang, and the few agents with non-zero probabilites of both gangs are confined to the honest-rich frontier. For decreasing values of β, the probabilities of being honest for agents inside the aggregates decrease until a certain threshold value β_c at which they disappear completely. It is also worth noting that the overall probability of finding a criminal inside each aggregate decreases as β increases because of this phenomenon of penetration of honest agents into the aggregates, and is not due to the appearance of the competitor gang, which never invades the rival aggregate.

The segregation of competing gangs into spatially separated aggregates makes mutual delation between gangs negligeable, so that the feature that differentiates HCCO and HCO dynamics seems to disappear. On the other hand, selective delation by honest agents provides a stabilizing mechanism for the persistence of both gangs: The size of the minority gang aggregate will increase respect to the size of the majority gang aggregate, so that the survival of equal size aggregates is guaranteed. In this situation, both gangs are delated by honest agents with equal probability, and then one is led to the idea that the dynamics in the interior of the aggregates is that of the HCO model.

A further support of this suggestion is provided by the fact that the value of the parameter β above which honest agents penetrate into the aggregates almost exactly coincides with the value β_c for the honesty transition of the HCO model, as shown in Figure 6a. The small excess (in both Markov and MC results) of honest agents for $\beta < \beta_c \approx 0.26$ is just due to the effect of the frontier between aggregates, where delation processes can (and they do) occur.

For $\beta > \beta_c$, as the penetration of honest agents into the aggregates increases, the Markov results for the HCCO model becomes progressively closer to the HCO results. To show this, we compute the probability distribution of being honest for certain values of α and β by building histograms showing honesty probabilities ρ_h of all agents of a given configuration. These histograms, shown in Figures 7b-c, are highly peaked at the HCO value both below and above β_c. The tails of the histograms reflect the existence of the frontier separating the gangs aggregates, whose effects become negligeable at higher values of β due to the abundance of honest agents inside the aggregates. We can conclude that the segregation of rival gangs leads the system to the behavior of the HCO model,

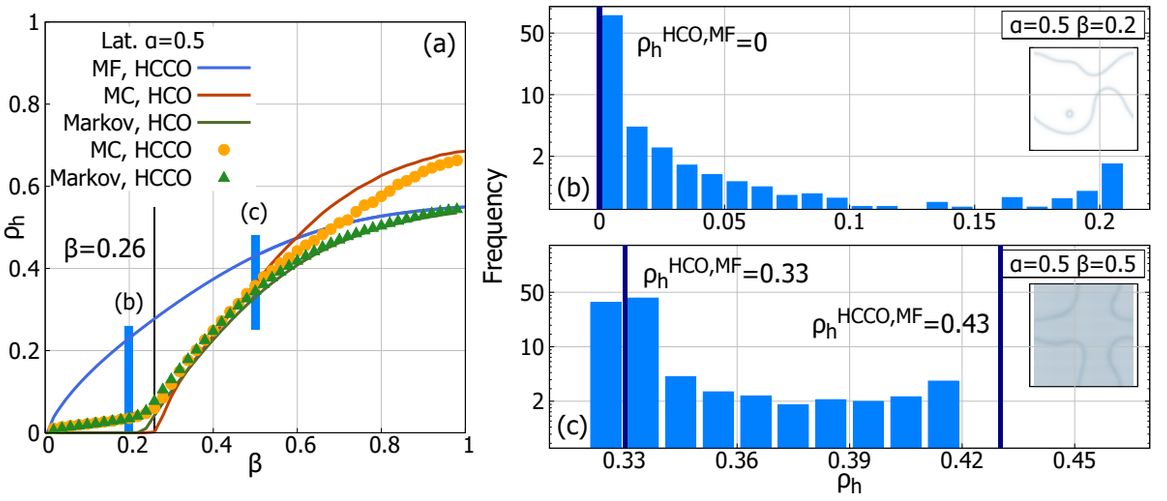

FIG. 6: Lattice. (a) Fraction of honest population as a function of β for $\alpha = 0.5$. mean-field results (blue line), Markov simulations (green triangles) and Monte Carlo simulations (orange circles) for HCCO model are shown, together with their counterparts in HCO model (green line for Markov and red line for Monte Carlo). The black vertical lines indicates the stability transition in HCO model for lattices $\beta_c = 0.26$, while blue rectangles indicate two different choices of β values, above and below β_c, where the Markov distributions of probabilities in the network are studied (panels b and c). In particular, the distribution of probabilities of each agent belonging to the H compartment is obtained for the configurations shown in the respective insets: (b) histogram for $\alpha = 0.5$ and $\beta = 0.2$, (c) histogram for $\alpha = 0.5$ and $\beta = 0.5$. Vertical dark blue lines indicate the value of ρ_h obtained with mean-field in the HCO model ($\rho_h^{\mathrm{HCO,MF}}$) and in the HCCO model ($\rho_h^{\mathrm{HCCO,MF}}$).

with small corrections due to boundary (between gangs) effects.

Regarding the MC dynamics, we see that, well after the penetration of honest agents into the gangs aggregates, the fraction of honest agents is significantly lower than in the HCO model. Though the rival gangs sizes are kept equal by the selective delation by honest agents, the MC stochastic fluctuations around the equal size situation effectively decrease the number of delations respect to the HCO model, and the fraction of honest agents becomes lower. In this case, segregation turns the (mean-field) advantage of honesty introduced by the selective delation strategy into a disadvantage. In lattices, non-selective delation can do better for $\beta > \beta_c$.

Segregation on Random Regular Networks

We have seen how the phenomenon of gangs segregation effectively transforms the HCCO model on lattices into an HCO with small corrections, providing an accurate explanation for the observed deviations (for both, Markov and MC dynamics) from mean-field predictions. As segregation occurs also in RRN networks, one should ask whether the observed deviations in these networks can also be explained along the same lines, i.e. as the effects of the emergence of subnetworks of HCO behavior.

In Figure 7a we show, for both Markov and MC dynamics on RRN, the fraction of honest agents $\rho_h(\beta)$ for fixed value of $\alpha = 0.5$. First of all, we see that there is no noticeable change of behavior near $\beta = \beta_c$, which casts serious doubts on the relationship between this behavior and the HCO model. Regarding the Markov behavior, we observe in the histograms of Figure 7b that the agents honesty probabilities clearly deviate from the HCO values. In Figure 7c, where $\beta = 0.5$, there is no segregation at all (see Figure 3), and all the nodes have the same population fractions predicted by mean-field. These results could have been expected from Figure 3, where one sees that, in RRN, both gangs are much more exposed to mutual delation than in lattices. We conclude that, in RRN, there are no subnetworks where the dynamics is HCO. Even when segregation into rival gangs aggregates occurs in RRN, its effects are quite different from those in lattices.

What explains the striking differences between lattices and RRN regarding the effects of segregation is the size of the frontiers that separate aggregates, and, in particular, the distance between any agent and those frontiers, as we now argue after the inspection of Figure 8. In this Figure we show, for RRN and lattices, the mean shortest distance d_{xy} between corrupt agents of species x and y ($x, y \in \{C_{in}, C_{st}\}$), defined as the average length of the shortest path from every agent x to the nearest agent y. Note that $d_{x,y} \geq 1$ always and, in general, $d_{c_{in},c_{st}} \neq d_{c_{st},c_{in}}$, and $d_{c_{in},c_{in}} \neq d_{c_{st},c_{st}}$, but they are approximately equal given the simmetry of the system, so we only show the distances $d_{c_{in},c_{st}}$ and $d_{c_{in},c_{in}}$ for clarity. When $x \neq y$, we effectively measure the distance to the nearest frontier (and thus, the size of the aggregate). We see that there are clear differences between the distances measured in RRN, that hardly reach values larger than 2, and those measured in lattices. Small distances means that every criminal has members of the opposing gang in its vicinity, and therefore, the mechanism of inter-gang delation comes often into play, preventing the emergence of the HCO behavior. This is what happens in

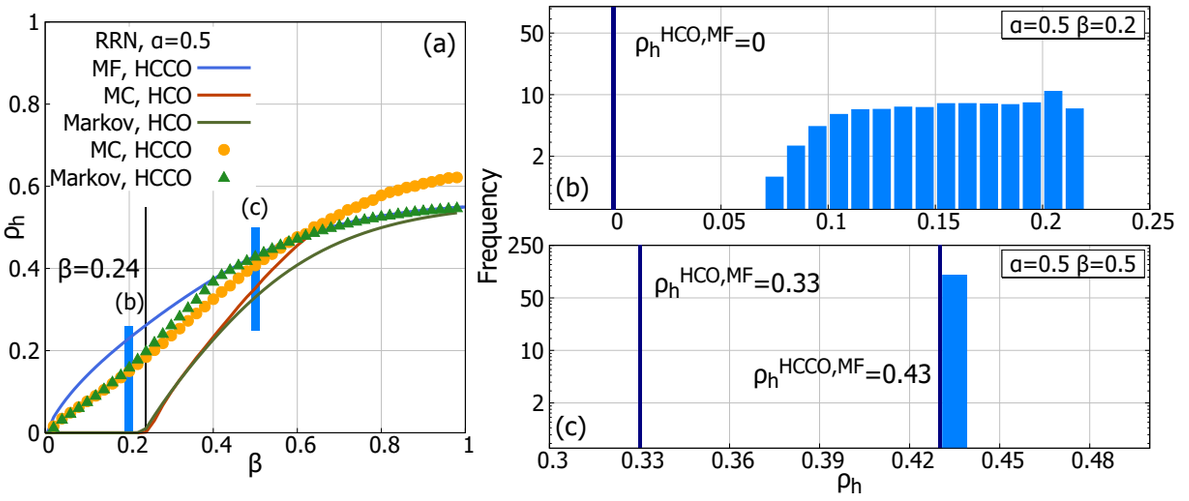

FIG. 7: Random regular network (RRN). (a) Fraction of honest population as a function of β for $\alpha = 0.5$. mean-field results (blue line), Markov simulations (green triangles) and Monte Carlo simulations (orange circles) for HCCO model are shown, together with their counterparts in HCO model (green line for Markov and red line for Monte Carlo). The black vertical lines indicates the stability transition in HCO model for RRN $\beta_c = 0.24$, while blue rectangles indicate two different choices of β values, above and below β_c, where the Markov distributions of probabilities in the network are studied (panels b and c). In particular, the distribution of probabilities of each agent belonging to the H compartment is obtained for two equilibrium configurations: (b) histogram for $\alpha = 0.5$ and $\beta = 0.2$, (c) histogram for $\alpha = 0.5$ and $\beta = 0.5$. Vertical dark blue lines indicates the value of ρ_h obtained with mean-field in the HCO model ($\rho_h^{\mathrm{HCO,MF}}$) and in the HCCO model ($\rho_h^{\mathrm{HCCO,MF}}$). In panel (c) we observe the situation where all nodes have the same honest probability, which corresponds to the mean-field behavior for HCCO model.

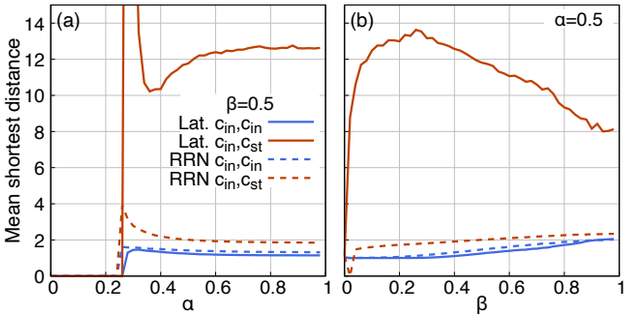

FIG. 8: Mean shortest distances between agents of opposing gangs (orange) and agents of the same gang (blue), for lattices (continous lines) and RRN (dashed lines). (a) Results for $\beta = 0.5$. (b) Results for $\alpha = 0.5$.

RRN, as we have seen before.

On the other hand, when distances increase, the inter-gang delation becomes rare and the prevailing mechanisms of the systems are the same as in the HCO model. Essentially, greater distances mean greater regions in the network where only one gang is present, and thus, HCO behavior is developed (see Figures 4 and 5, where gangs aggregates are clearly visible). This is what happens in lattices, as can be seen in Figure 8, where inter-gang mean distances reach values up to 7, while intra-gang distances remain close to 1.

Differences in behavior between networks come from their structural features: spatial correlations inherent to lattices result in much longer average shortest path lengths and diameters than in RRN, where the small world property brings all agents together. Therefore, networks with longer average distances allow for the partitioning of the network between both gangs, which rarely interact, while networks with small-world property promote inter-gang interactions, effectively dragging all agents to the frontiers. Although segregation is also present and plays an important role in the asymptotic composition of the system, it is not sufficient to break the HCCO model into two HCO models.

III. CONCLUDING REMARKS

In this work we have proposed a generalization of the HCO model formulated in reference[1] to explore the prevalence of crime in a given society under the coexistence and competition impact of two different opposing gangs.

The mean-field analysis of the model reveals the existence of different equilibria as a function of the delation mechanism of the honest population. While non-selective delation always leads to the extinction of the minority gang, the introduction of a selective delation, reducing the probability that honest agents delate the minority gang, leads to a coexistence regime. As a result of the inter-gang delation events, the latter choice turns into a convenient strategy, leading to a lower penetration of crime than in the former scenario.

To characterize the evolution of crime in networked populations, we have proposed a set of Markov equations which are

validated through extensive agent-based Monte Carlo simulations. Regarding the impact of the coexistence of two gangs, we have found a pretty different qualitative picture from that predicted by the mean-field theory, leading to a higher penetration of crime in some regions of the parameter space. Quantitatively, these differences strongly depend on the structural features of the underlying network, becoming more relevant for spatially structured configurations.

The fact that the Markov dynamics results, starting with heterogeneous initial conditions, differ from the mean-field theory and approach to the Monte Carlo simulations is rarely observed in regular networks for these kind of models. The presence of both competing gangs seems to preserve and even amplify the initial heterogeneities of the fraction of species in the system.

To unveil the underlying phenomena that produce this disagreement we proposed a new segregation measure and studied the distances separating the different gangs. Regardless of the underlying network, we found that agents' surroundings substantially differ from the well-mixed scenario, resulting in segregation between both gangs. Moreover, in networks with spatial structure, this segregation plays a major role, leading to the emergence of two disjoint macroscopic clusters of criminals, each one associated with a gang. The size of these clusters, quantified with the inter-gang distances, is large enough to impair the cross delation events, thus explaining the important differences found with respect to the mean-field predictions.

In general terms, our analysis reveals that the interplay of the network structure, the competition between spreading units (criminal gangs) and the strategy chosen to control their diffusion (delation mechanism) crucially shapes the outcome of the dynamics. Along this line, we have proposed simple microscopic rules which amplify small local perturbations to give rise to macroscopic collective behaviors. This work, albeit limited in scope, lays the foundation for the ellaboration of a more complete formalism that overcomes some of its intrinsic limitations. Namely, it does not contemplate the existence of pure, incorruptible agents, other realistic features inherent to corruption such as the lack of reinsertion of certain individuals[55] and social stigma[56–58], or the fact that gang recruitment can be often subordinated to the sharing of cultural or racial traits that may prevent an agent from being corrupted into a certain gang[48]. Moreover, repressive action is not explicitly taken into account, as corrupt agents cannot spontaneously reach Ostracism. Similar mechanisms, like warning to wrongdoers or social intimidation effects have been previously included[1,2] but not explicitly incorporated here in order to clearly analyze the effect of gang competition. Nonetheless, we hope that this work will inspire future research on competing dynamics as well, such as the spread of opposite ideas in social networks[59,60].

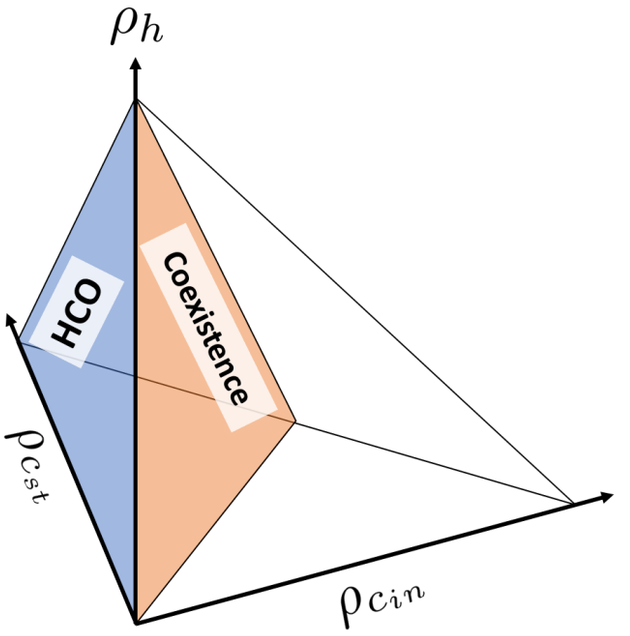

FIG. 9: Diagram representing the state-space for HCCO model. Blue surface: region where HCO behavior takes place. In this case, we have selected the $\rho_{c_{in}} = 0$ face, but the other face of the tetrahedron ($\rho_{c_{st}} = 0$) also develops the HCO behavior. Orange surface: both corrupt gangs coexistence region with the same fraction $\rho_{c_{in}} = \rho_{c_{st}}$.

ACKNOWLEDGMENTS

We acknowledge financial support from grant PID2020-113582GB-I00 funded by MCIN/AEI/10.13039/501100011033, and from Departamento de Industria e Innovación del Gobierno de Aragón y Fondo Social Europeo through projects no. E30_17R (COMPHYS group) and E36_17R (FENOL group). H.P.M. and F.B. acknowledge financial support from Gobierno de Aragón through doctoral fellowships. F.B. acknowledges financial support from Spanish Ministerio de Ciencia e Innovación (grant PGC2018-094684-B-C22).

DATA AVAILABILITY STATEMENT

Data sharing is not applicable to this article as no new data were created or analyzed in this study.

Appendix A: Mean-field analysis of the HCCO model

We will analyze here the asymptotic behavior for the mean-field approximation of the HCCO model, For the choice of non-selective delation rates, where honest agents delate both gangs with an equal probability, we arrive to the result that both gangs cannot coexist. However, for the case of selective delation a state of coexistence of the gangs is stable with a large basin of attraction. Moreover, the fraction of honest agents in the population for this state of gangs' coexistence is significantly higher than that of the HCO (single-gang) model for the same values of the model parameters (i.e., α, β, r).

The mean-field approximation is based on the assumption of homogeneity of both, field (agent state; H, C_{in}, C_{st} or O), and structure of contacts (adjacency matrix $\mathbf{A}$). Under these circumstances, it seems plausible considering average behavior as a good (least biased) estimation of agent's behavior, i.e.: $\vec{\rho}(i) = \langle \vec{\rho} \rangle$ (for all i) for the associated Markov process, and the neighborhood of size k can be selected at random among the population at each time step. Therefore, by using the normalization condition, the mean-field discrete time dynamics becomes a non linear three-dimensional map of the simplex (tetrahedron, shown in Figure 9) $\mathscr{S}_3$ (*i.e.*: $0 \leq \rho_h, \rho_{c_{in}}, \rho_{c_{st}} \leq 1$, $\rho_h + \rho_{c_{in}} + \rho_{c_{st}} \leq 1$) onto itself, if one chooses ρ_h, $\rho_{c_{in}}$ and $\rho_{c_{st}}$ as independent variables.

One associates to this map a three-dimensional flow (continuous time dynamics) defined by the velocity (3d vector) field $\vec{F}(\vec{\rho})$, on the simplex

$$\vec{F}(\vec{\rho}) = \dot{\vec{\rho}} \equiv (\dot{\rho}_h, \dot{\rho}_{c_{in}}, \dot{\rho}_{c_{st}})$$

whose components are:

$$\begin{aligned} F_h(\vec{\rho}) &= -f_\alpha \rho_h + r\rho_o = -[f_\alpha + r]\,\rho_h + r\,[1 - (\rho_{c_{in}} + \rho_{c_{st}})] \ , \\ F_{c_{in}}(\vec{\rho}) &= f_\alpha\, t(\rho_{c_{in}}, \rho_{c_{st}})\, \rho_h - f_\beta^{in}\, \rho_{c_{in}} \ , \\ F_{c_{st}}(\vec{\rho}) &= f_\alpha\, t(\rho_{c_{st}}, \rho_{c_{in}})\, \rho_h - f_\beta^{st}\, \rho_{c_{st}} \ , \end{aligned} \tag{A1}$$

where, in this mean-field approximation, the corruption rate is given by

$$f_\alpha = 1 - [1 - \alpha(\rho_{c_{in}} + \rho_{c_{st}})]^k \ , \tag{A2}$$

and the delation rates are

$$\begin{aligned} f_\beta^{in} &= 1 - [1 - \beta(\rho_h B(\rho_{c_{in}}, \rho_{c_{st}}) + \rho_{c_{st}})]^k \ , \\ f_\beta^{st} &= 1 - [1 - \beta(\rho_h B(\rho_{c_{st}}, \rho_{c_{in}}) + \rho_{c_{in}})]^k \ . \end{aligned} \tag{A3}$$

where $B(x,y) = 1$ for the non-selective delation scenario, while it is given by (7) for the selective delation one.

For both cases, one easily sees that the velocity field $\vec{F}(\vec{\rho})$ satisfies the symmetry

$$F_{c_{in}}(\rho_h, \rho_{c_{in}}, \rho_{c_{st}}) = F_{c_{st}}(\rho_h, \rho_{c_{st}}, \rho_{c_{in}}) \ , \tag{A4}$$

and thus the phase portrait posseses mirror symmetry respect to the two-dimensional surface $\rho_{c_{in}} = \rho_{c_{st}}$ (bisector plane). As a consequence, the bisector plane is an invariant set. It is easy to check that there are two additional invariant 2d surfaces, namely the single-gang faces, $\rho_{c_{in}} = 0$ and $\rho_{c_{st}} = 0$.

The dynamics on the single-gang face $\rho_{c_y} = 0$ ($y = in, st$) is that of the HCO model[1], whose asymptotic behavior we summarize as follows: For fixed values of the parameters α, β, and r there is a unique attractor of the face trajectories (no multi-stability).

- If $\alpha < \alpha_c = \frac{1-(1-\beta)^k}{k}$ then the full honesty state, i.e. the vertex $\rho_h = 1$, is the attractor.
- If $\beta < \beta_c = \frac{1-(1-\alpha)^k}{k}$ then the full corruption state, i.e. the vertex $\rho_{c_x} = 1$, is the attractor.

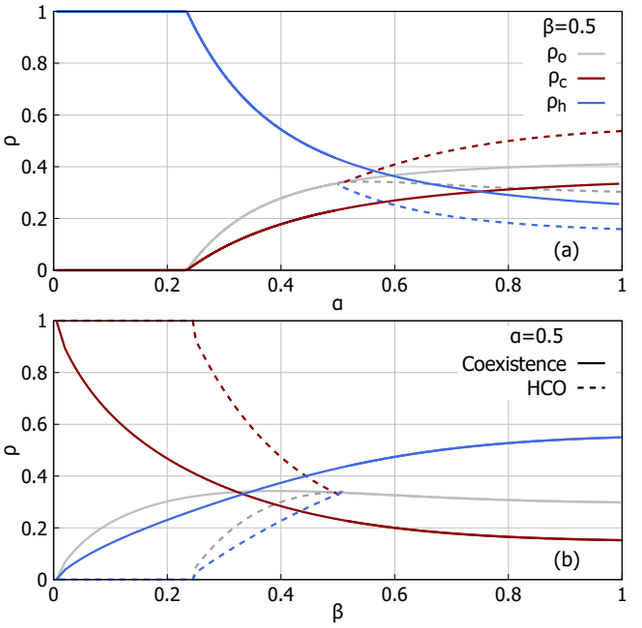

FIG. 10: Fraction of honest (blue), total penetration of crime (red) and ostracism (grey) population in equilibrium, for $r = 0.5$, $k = 4$. (a) mean-field results for $\beta = 0.5$, as function of α. (b) mean-field results for $\alpha = 0.5$, as function of β. Solid lines correspond to the state of coexistence of competing gangs and dashed lines to the state of a single gang survival.

- If $\alpha > \alpha_c = \frac{1-(1-\beta)^k}{k}$ and $\beta > \beta_c = \frac{1-(1-\alpha)^k}{k}$, there is an interior attractor $(\bar{\rho}_h, \bar{\rho}_{c_x})$ which is the solution of the non-linear equations

$$\begin{aligned} F_h(\vec{\rho}) &= -[f_\alpha + r]\,\bar{\rho}_h + r\,[1 - \bar{\rho}_{c_x}] = 0 \ , \\ F_{c_x}(\vec{\rho}) &= f_\alpha\, \bar{\rho}_h - f_\beta^x\, \bar{\rho}_{c_x} = 0 \ , \end{aligned} \tag{A5}$$

  where f_α is given by (*A*2), and f_β^x by (*A*3), evaluated at $(\bar{\rho}_h, \bar{\rho}_{c_x})$.

The dynamics on the bisector plane $\rho_{c_{in}} = \rho_{c_{st}} = \rho_c$ shows some differences. The full corruption state in the single-gang HCO (that is now $2\rho_c = 1$) is no longer a fixed point, due to the mutual delation of the gangs. We have now only two scenarios for the restriction of the phase portrait to this invariant set:

- If $\alpha < \alpha_c = \frac{1-(1-\beta)^k}{k}$ then the full honesty state, i.e. the vertex $\rho_h = 1$, is the attractor.
- If $\alpha > \alpha_c = \frac{1-(1-\beta)^k}{k}$ then there is an interior attractor (ρ_h^*, ρ_c^*) of the face trajectories, which is the solution of the non-linear equations

$$\begin{aligned} F_h(\vec{\rho}) &= -[f_\alpha + r]\,\rho_h^* + r\,[1 - 2\rho_c^*] = 0 \ , \\ F_{c_x}(\vec{\rho}) &= f_\alpha\, \rho_h^* - f_\beta^x\, \rho_c^* = 0 \end{aligned} \tag{A6}$$

  where the rates f_α and f_β^x are evaluated at (ρ_h^*, ρ_c^*).

Now, it must be realized that being attractor (stable fixed point) of the trajectories inside a 2d invariant set does not

guarantee its attractor character on the 3d phase space, because perturbations out of the invariant set could destabilize the fixed point under consideration. It turns out that, in this respect, the selective (or not) character of the delation by honest agents makes an important difference. The population fractions in the equilibrium both in the coexistence case $(\bar{\rho}_h, \bar{\rho}_{c_{in}}, \bar{\rho}_{c_{st}})$ (bisector plane) and the single-gang HCO case (ρ_h^*, ρ_c^*) (face plane) are shown in Figure 10. Note that the total honest population is always greater in the case of coexistence, due to the cross-delation processes between gangs.

Non-selective delation

For the non-selective delation scenario, and $\alpha > \alpha_c$, when a small perturbation $\delta\vec{\rho} = (\delta\rho_h = 0, \delta\rho_{c_x} = -\varepsilon, \delta\rho_{c_y} = \varepsilon)$ is applied to the single-gang face fixed point $(\bar{\rho}_h, \bar{\rho}_{c_x})$, the linearized equation of motion for the minority gang fraction is obtained, after some simple algebra, as

$$\dot{\rho}_{c_y} = \varepsilon \left[(1 - \beta(\bar{\rho}_h + \bar{\rho}_{c_x}))^k - (1 - \beta(\bar{\rho}_h))^k \right] < 0 \,, \qquad \text{(A7)}$$

and thus the velocity field points toward the single-gang face, that attracts nearby trajectories. On the contrary, when the same perturbation is applied to the fixed point on the bisector plane (ρ_h^*, ρ_c^*), making C_x minority, the linearized equations become

$$\dot{\rho}_{c_y} = -\dot{\rho}_{c_x} = k\beta\varepsilon\rho_c^* \, (1 - \beta(\rho_h^* + \rho_c^*))^{k-1} > 0 \,, \qquad \text{(A8)}$$

and the perturbation is amplified away from the fixed point. Trajectories nearby the bisector plane flow away from it toward the single-gang face.

In summary, when honest agents delate both gangs with equal probability, the generic phase space trajectories evolve either toward the full honesty state, if $\alpha < \alpha_c$, or (otherwise) toward the attractor on one of the single-gang faces, that are "full C_{in}" and "full C_{st}" if $\beta < \beta_c$, or otherwise $(\bar{\rho}_h, \bar{\rho}_{c_{in}}, 0)$ and $(\bar{\rho}_h, 0, \bar{\rho}_{c_{st}})$. For $\alpha > \alpha_c$, the bisector plane is the basin boundary, i.e. the surface that divides the phase space in two basins of attraction.

Selective delation by honest agents

To simplify the linear stability analysis of both, single-gang and gang-coexistence fixed points, we will take the limit $T \to 0$ of the function $B(x,y)$ defined by equation (7):

$$\lim_{T\to 0} B(x,y) = \theta(x,y) = \begin{cases} 1 & \text{if } x \geq y \,, \\ 0 & \text{if } x < y \,. \end{cases} \qquad \text{(A9)}$$

This change does not modify the results of the analysis, while it considerably simplifies the mathematical arguments. Also, to alleviate the notation, we define a one-variable function $f_\beta(x) = 1 - (1 - \beta x)^k$, so that, if C_{in} is the majority gang, the equations A3 are reduced to

$$\begin{aligned} f_\beta^{in} &= f_\beta(\rho_h + \rho_{c_{st}}) \,, \\ f_\beta^{st} &= f_\beta(\rho_{c_{in}}) \,. \end{aligned} \qquad \text{(A10)}$$

By applying a small perturbation $\delta\vec{\rho} = (\delta\rho_h = 0, \delta\rho_{c_{in}} = \varepsilon, \delta\rho_{c_{st}} = -\varepsilon)$ to the fixed point $(\rho_h^*,\ \rho_{c_{in}}^* = \rho_c^*,\ \rho_{c_{st}}^* = \rho_c^*)$ on the bisector plane, the system is placed at $(\rho_h^*, \rho_c^* + \varepsilon, \rho_c^* - \varepsilon)$, where C_{in} is the majority gang, and we can use (A10). The linearized equations of motion for the gangs are:

$$\dot{\rho}_{c_{in}} = f_\beta(\rho_h^* + \rho_c^*)(\rho_c^* + \varepsilon) - f_\beta(\rho_h^* + \rho_c^* - \varepsilon)(\rho_c^* + \varepsilon) > 0 \,, \qquad \text{(A11)}$$

$$\dot{\rho}_{c_{st}} = f_\beta(\rho_h^* + \rho_c^*)(\rho_c^* - \varepsilon) - f_\beta(\rho_c^* + \varepsilon)(\rho_c^* - \varepsilon) > 0 \,. \qquad \text{(A12)}$$

Although $\rho_{c_{in}}$ increases, the velocity field points toward the bisector plane, because the increasing character of the function f_β and the condition $\varepsilon \ll 1$, ensures that $\dot{\rho}_{c_{st}} > \dot{\rho}_{c_{in}}$. Therefore, the flow will tend to restore the equilibrium situation, and the fixed point on the bisector becomes stable for any choice of α and β, provided $\alpha > \alpha_c$ (the condition for the existence of this fixed point). We see how the selective delation by honest agents, delating the minority gang with a lower (null, in the previous analysis, where B is a step function) probability reverses the stability of the state of gangs coexistence.

In this state of coexistence of competing gangs, the fraction of honest agents is significantly higher that in the single-gang state. The reason is that the mutual delation of opposing gangs, which is absent on the single-gang faces, decreases the total penetration of crime. In this scenario of strongly competing gangs, the selective delation by honest agents that leads to the survival of both gangs allows an additional source of delation, and thus it turns out to be a sort of efficient strategy against corruption.

Let us now consider the stability of the fixed point $(\bar{\rho}_h, \bar{\rho}_{c_{in}}, 0)$, interior to the $\rho_{c_{st}} = 0$ single-gang face, by adding a small perturbation $\delta\vec{\rho} = (\delta\rho_h = 0, \delta\rho_{c_{in}} = -\varepsilon, \delta\rho_{c_{st}} = \varepsilon)$, so that we can use (A10) at the pertubed state. After some simple algebra, the linearized equations of motion for the gangs are:

$$\dot{\rho}_{c_{in}} = \left[f_\beta(\bar{\rho}_h) - f_\beta(\bar{\rho}_h + \varepsilon) \right] (\bar{\rho}_c - \varepsilon) \,, \qquad \text{(A13)}$$

$$\dot{\rho}_{c_{st}} = \left[f_\beta(\bar{\rho}_h) - f_\beta(\bar{\rho}_c - \varepsilon) \right] \varepsilon \,. \qquad \text{(A14)}$$

The increasing character of the function f_β and the condition $\varepsilon \ll 1$, ensures that $\dot{\rho}_{c_{in}} < 0$. The direction of the velocity field at the perturbed state points toward the single-gang face if $\dot{\rho}_{c_{st}} < 0$, and we see that, at lowest order in ε, $\operatorname{sign} \dot{\rho}_{c_{st}} = \operatorname{sign}(\bar{\rho}_h - \bar{\rho}_{c_{in}})$. From the symmetry of the (single-gang) HCO model (in the absence of the warning to wrongdoers effect) analyzed in[1], we know that $\operatorname{sign}(\bar{\rho}_h - \bar{\rho}_{c_{in}}) = \operatorname{sign}(\beta - \alpha)$, and then if $\alpha < \beta$ the single-gang face fixed point is unstable, but becomes an attractor of nearby trajectories if $\alpha > \beta$. A more detailed analysis shows that this bifurcation is produced by the collision with a stable fixed point outside the phase space (for $\alpha < \beta$), that interchanges stability with the single-gang fixed point, then becoming unstable at its entrance into the phase space, when the single-gang fixed point becomes stable.

Summarizing the linear stability analysis for the selective delation case,

- If $\alpha < \alpha_c$ the unique asymptotic state is the full honesty state.

- If $\alpha_c < \alpha < \beta$, the unique asymptotic state is the gangs coexistence state $(\rho_h^*,\ \rho_{c_{in}}^* = \rho_c^*,\ \rho_{c_{st}}^* = \rho_c^*)$.

- If $\beta < \alpha$ there are three attractors for the dynamics, namely the state of equally populated gangs in the bisector plane, and the two single-gang states in the invariant faces on the boundary. The size of the basins of attraction for the latter increases as α increases. Moreover, for values of the parameter $\beta < 1/k$, there is a value of the parameter $\alpha = \alpha^*$, defined by the condition $\beta_c(\alpha^*) = \beta$, such that if $\alpha^* < \alpha$, the single-gang states are the full C states.

REFERENCES

[1]D. Lu, F. Bauza, D. Soriano-Paños, J. Gómez-Gardeñes, and L. Floría, "Norm violation versus punishment risk in a social model of corruption," Physical Review E **101**, 022306 (2020).
[2]F. Bauzauthor D. Soriano-Pa
, J. G-Garde
, and L. M. Floría, "Fear induced explosive transitions in the dynamics of corruption," Chaos: An Interdisciplinary Journal of Nonlinear Science **30**, 063107 (2020).
[3]R. Axelrod and W. D. Hamilton, "The evolution of cooperation," science **211**, 1390–1396 (1981).
[4]H. Gintis, *Game theory evolving* (Princeton university press, 2009).
[5]C. F. Camerer, *Behavioral game theory: Experiments in strategic interaction* (Princeton university press, 2011).
[6]C. Castellano, S. Fortunato, and V. Loreto, "Statistical physics of social dynamics," Reviews of modern physics **81**, 591 (2009).
[7]G. Szabó and G. Fath, "Evolutionary games on graphs," Physics reports **446**, 97–216 (2007).
[8]C. P. Roca, J. A. Cuesta, and A. Sánchez, "Evolutionary game theory: Temporal and spatial effects beyond replicator dynamics," Physics of life reviews **6**, 208–249 (2009).
[9]M. Perc, J. G-Garde
, A. Szolnoki, L. M. Floría, and Y. Moreno, "Evolutionary dynamics of group interactions on structured populations: A review," Journal of The Royal Society Interface **10**, 20120997 (2013).
[10]R. Axelrod, "The dissemination of culture: A model with local convergence and global polarization," Journal of conflict resolution **41**, 203–226 (1997).
[11]A. Baronchelli, "The emergence of consensus: a primer," Royal Society open science **5**, 172189 (2018).
[12]M. Granovetter, "Threshold models of collective behavior," American journal of sociology **83**, 1420–1443 (1978).
[13]D. Watts, "A simple model of global cascades on random networks." Proceedings of the National Academy of Sciences of the United States of America **99**, 5766–5771 (2002).
[14]J. G-Garde L. Lotero, S. Taraskin, and F. Pz-Reche, "Explosive contagion in networks," Scientific reports **6**, 1–9 (2016).
[15]F. Baumann, P. Lorenz-Spreen, I. M. Sokolov, and M. Starnini, "Modeling echo chambers and polarization dynamics in social networks," Physical Review Letters **124**, 048301 (2020).
[16]D. Lazer, A. S. Pentland, L. Adamic, S. Aral, A. L. Barabasi, D. Brewer, N. Christakis, N. Contractor, J. Fowler, M. Gutmann, *et al.*, "Life in the network: the coming age of computational social science," Science (New York, NY) **323**, 721 (2009).
[17]R. Conte, N. Gilbert, G. Bonelli, C. Cioffi-Revilla, G. Deffuant, J. Kertesz, V. Loreto, S. Moat, J.-P. Nadal, A. Sanchez, *et al.*, "Manifesto of computational social science," The European Physical Journal Special Topics **214**, 325–346 (2012).
[18]D. M. Lazer, A. Pentland, D. J. Watts, S. Aral, S. Athey, N. Contractor, D. Freelon, S. Gonzalez-Bailon, G. King, H. Margetts, *et al.*, "Computational social science: Obstacles and opportunities," Science **369**, 1060–1062 (2020).
[19]J. M. Hofman, D. J. Watts, S. Athey, F. Garip, T. L. Griffiths, J. Kleinberg, H. Margetts, S. Mullainathan, M. J. Salganik, S. Vazire, *et al.*, "Integrating explanation and prediction in computational social science," Nature **595**, 181–188 (2021).
[20]J.-P. Onnela, J. Saramäki, J. Hyvönen, G. Szabó, D. Lazer, K. Kaski, J. Kertész, and A.-L. Barabási, "Structure and tie strengths in mobile communication networks," Proceedings of the national academy of sciences **104**, 7332–7336 (2007).
[21]P. Grindrod and T. Lee, "Comparison of social structures within cities of very different sizes," Royal Society open science **3**, 150526 (2016).
[22]A. B. Migliano, A. E. Page, J. Gómez-Gardeñes, G. D. Salali, S. Viguier, M. Dyble, J. Thompson, N. Chaudhary, D. Smith, J. Strods, *et al.*, "Characterization of hunter-gatherer networks and implications for cumulative culture," Nature Human Behaviour **1**, 1–6 (2017).
[23]D. Mistry, M. Litvinova, A. P. y Piontti, M. Chinazzi, L. Fumanelli, M. F. Gomes, S. A. Haque, Q.-H. Liu, K. Mu, X. Xiong, *et al.*, "Inferring high-resolution human mixing patterns for disease modeling," Nature communications **12**, 1–12 (2021).
[24]M. C. Gonzalez, C. A. Hidalgo, and A.-L. Barabasi, "Understanding individual human mobility patterns," nature **453**, 779–782 (2008).
[25]L. Alessandretti, U. Aslak, and S. Lehmann, "The scales of human mobility," Nature **587**, 402–407 (2020).
[26]H. Barbosa, M. Barthelemy, G. Ghoshal, C. R. James, M. Lenormand, T. Louail, R. Menezes, J. J. Ramasco, F. Simini, and M. Tomasini, "Human mobility: Models and applications," Physics Reports **734**, 1–74 (2018).
[27]L. Lotero, R. G. Hurtado, L. M. Floría, and J. Gómez-Gardeñes, "Rich do not rise early: spatio-temporal patterns in the mobility networks of different socio-economic classes," Royal Society open science **3**, 150654 (2016).
[28]G. Tóth, J. Wachs, R. Di Clemente, Á. Jakobi, B. Ságvári, J. Kertész, and B. Lengyel, "Inequality is rising where social network segregation interacts with urban topology," Nature communications **12**, 1–9 (2021).
[29]C. Gracia-Lázaro, A. Ferrer, G. Ruiz, A. Tarancón, J. A. Cuesta, A. Sánchez, and Y. Moreno, "Heterogeneous networks do not promote cooperation when humans play a prisoner?s dilemma," Proceedings of the National Academy of Sciences **109**, 12922–12926 (2012).
[30]M. Karsai, G. Iniguez, K. Kaski, and J. Kertész, "Complex contagion process in spreading of online innovation," Journal of The Royal Society Interface **11**, 20140694 (2014).
[31]J. Poncela-Casasnovas, M. Gutiérrez-Roig, C. Gracia-Lázaro, J. Vicens, J. Gómez-Gardeñes, J. Perelló, Y. Moreno, J. Duch, and A. Sánchez, "Humans display a reduced set of consistent behavioral phenotypes in dyadic games," Science advances **2**, e1600451 (2016).
[32]D. Centola, J. Becker, D. Brackbill, and A. Baronchelli, "Experimental evidence for tipping points in social convention," Science **360**, 1116–1119 (2018).
[33]A. Szekely, F. Lipari, A. Antonioni, M. Paolucci, A. Sánchez, L. Tummolini, and G. Andrighetto, "Evidence from a long-term experiment that collective risks change social norms and promote cooperation," Nature communications **12**, 1–7 (2021).
[34]K. Faust and G. E. Tita, "Social Networks and Crime: Pitfalls and Promises for Advancing the Field," Annual Review of Criminology **2**, 99–122 (2019).
[35]I. Villamil, J. Kert, and J. Wachs, "Computational Approaches to the Study of Corruption," arXiv:2201.11880 [physics] (2022), arXiv: 2201.11880.
[36]B. Green, T. Horel, and A. V. Papachristos, "Modeling Contagion Through Social Networks to Explain and Predict Gunshot Violence in Chicago, 2006 to 2014," JAMA Internal Medicine **177**, 326–333 (2017).
[37]S. Abdulrahman, "Stability analysis of the transmission dynamics and control of corruption," Pacific Journal of Science and Technology **15**, 99–113 (2014).
[38]S. Hathroubi and H. Trabelsi, "Epidemic Corruption: A Bio-Economic Homology," European Scientific Journal **10**, 228–235 (2014).
[39]P. Blanchard, A. Krüger, T. Krueger, and P. Martin, "The epidemics of corruption," arXiv preprint physics/0505031 (2005).
[40]J.-H. Lee, Y. Iwasa, U. Dieckmann, and K. Sigmund, "Games of corruption: How to suppress illegal logging," Proceedings of the National Academy of Sciences **116**, 13276–13281 (2019).
[41]J.-H. Lee, K. Sigmund, U. Dieckmann, and Y. Iwasa, "Games of corruption: How to suppress illegal logging," Journal of Theoretical Biology **367**, 1–13 (2015).
[42]V. Kolokoltsov and O. Malafeyev, "Mean-field-game model of corruption,"

Dynamic Games and Applications **7**, 34–47 (2017).
[43]P. Verma and S. Sengupta, "Bribe and punishment: An evolutionary game-theoretic analysis of bribery," PLoS ONE **10**, e0133441 (2015).
[44]R. Axelrod, "An evolutionary approach to norms," American political science review **80**, 1095–1111 (1986).
[45]J. L. Coleman, "The rational choice approach to legal rules," Chi.-Kent L. Rev. **65**, 177 (1989).
[46]A. Cardillo, J. Gómez-Gardeñes, D. Vilone, and A. Sánchez, "Co-evolution of strategies and update rules in the prisoner's dilemma game on complex networks," New Journal of Physics **12**, 103034 (2010).
[47]F. Battiston, G. Cencetti, I. Iacopini, V. Latora, M. Lucas, A. Patania, J.-G. Young, and G. Petri, "Networks beyond pairwise interactions: structure and dynamics," Physics Reports **874**, 1–92 (2020).
[48]J. Gravel, B. Allison, J. West-Fagan, M. McBride, and G. E. Tita, "Birds of a Feather Fight Together: Status-Enhancing Violence, Social Distance and the Emergence of Homogenous Gangs," Journal of Quantitative Criminology **34**, 189–219 (2018).
[49]G. DeAngelo, "Making space for crime: A spatial analysis of criminal competition," Regional Science and Urban Economics **42**, 42–51 (2012).
[50]G. E. Tita and R. T. Greenbaum, "Crime, Neighborhoods, and Units of Analysis: Putting Space in Its Place," in *Putting Crime in its Place: Units of Analysis in Geographic Criminology*, edited by D. Weisburd, W. Bernasco, and G. J. Bruinsma (Springer, New York, NY, 2009) pp. 145–170.
[51]G. E. Tita and S. M. Radil, "Spatializing the Social Networks of Gangs to Explore Patterns of Violence," Journal of Quantitative Criminology **27**, 521–545 (2011).
[52]P. J. Brantingham, M. Valasik, and G. E. Tita, "Competitive dominance, gang size and the directionality of gang violence," Crime Science **8**, 7 (2019).
[53]P. J. Brantingham, G. E. Tita, M. B. Short, and S. E. Reid, "The ecology of gang territorial boundaries," Criminology **50**, 851–885 (2012).
[54]S. Gómez, A. Arenas, J. Borge-Holthoefer, S. Meloni, and Y. Moreno, "Discrete-time markov chain approach to contact-based disease spreading in complex networks," EPL (Europhysics Letters) **89**, 38009 (2010).
[55]H. V. Ribeiro, L. G. Alves, A. F. Martins, E. K. Lenzi, and M. Perc, "The dynamical structure of political corruption networks," Journal of Complex Networks **6**, 989–1003 (2018).
[56]D. G. Rand, S. Arbesman, and N. A. Christakis, "Dynamic social networks promote cooperation in experiments with humans," Proceedings of the National Academy of Sciences **108**, 19193–19198 (2011).
[57]X.-W. Wang, L.-L. Jiang, S. Nie, S.-M. Chen, and B.-H. Wang, "Promoting cooperation through fast response to defection in spatial games," New Journal of Physics **18**, 103025 (2016).
[58]C. Gracia-Lázaro, F. Quijandría, L. Hernández, L. M. Floría, and Y. Moreno, "Coevolutionary network approach to cultural dynamics controlled by intolerance," Physical Review E **84**, 067101 (2011).
[59]M. Cinelli, G. D. F. Morales, A. Galeazzi, W. Quattrociocchi, and M. Starnini, "The echo chamber effect on social media," Proceedings of the National Academy of Sciences **118** (2021).
[60]W. Cota, S. C. Ferreira, R. Pastor-Satorras, and M. Starnini, "Quantifying echo chamber effects in information spreading over political communication networks," EPJ Data Science **8**, 1–13 (2019).

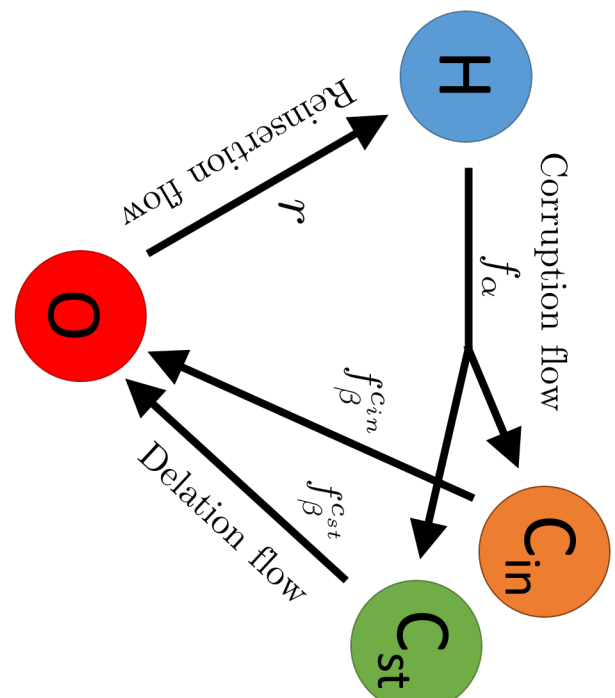

Chaos

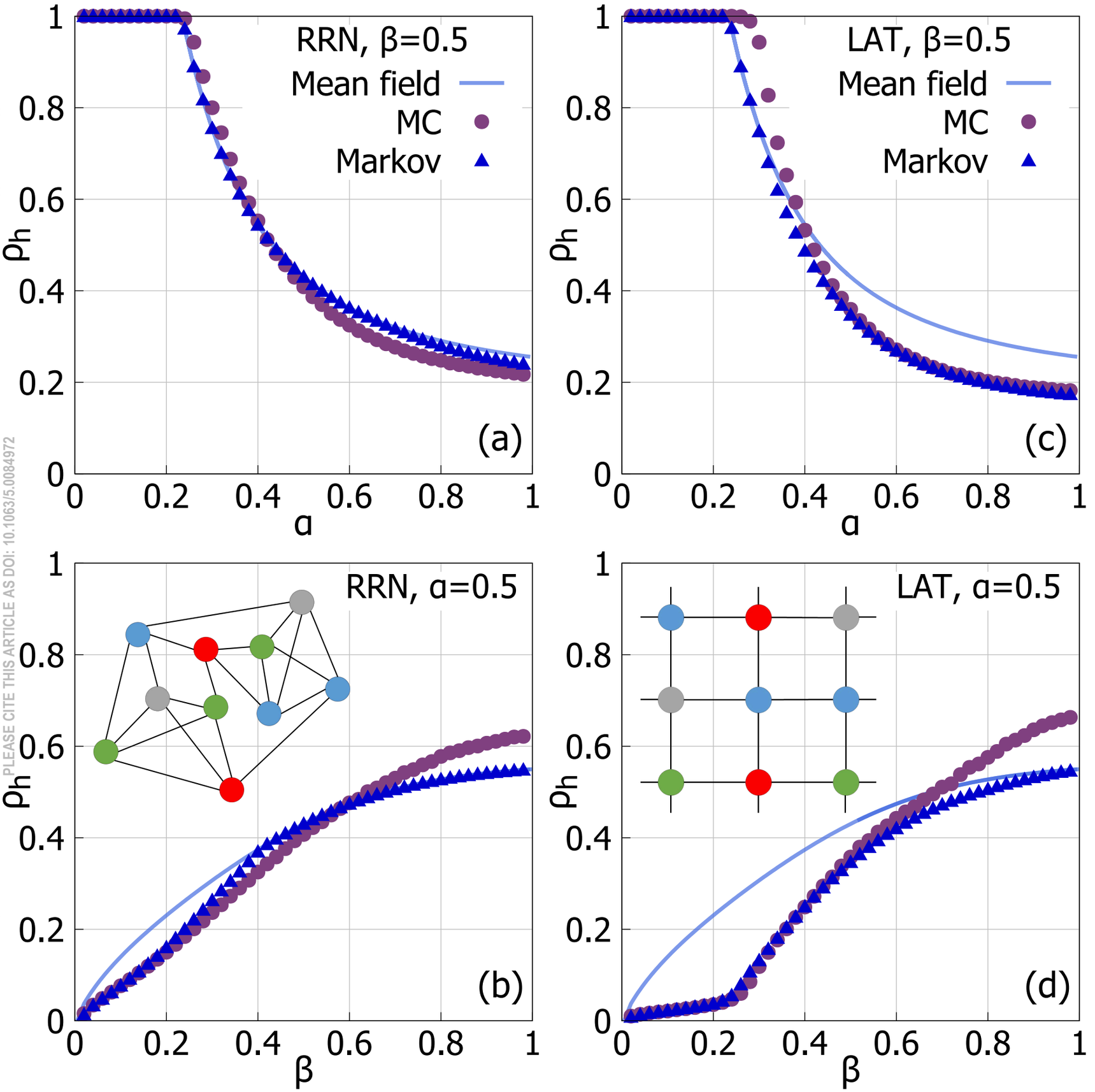

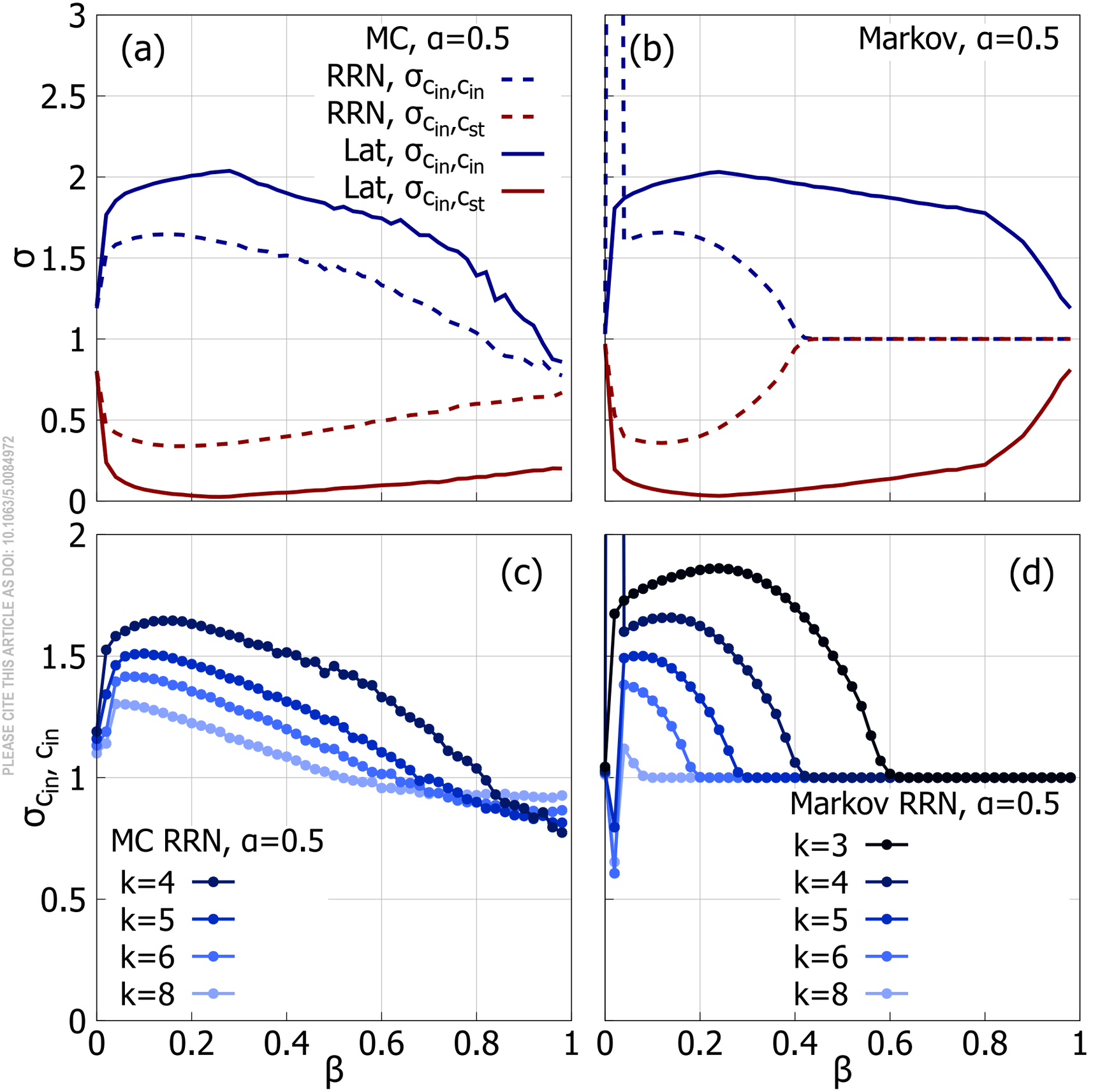

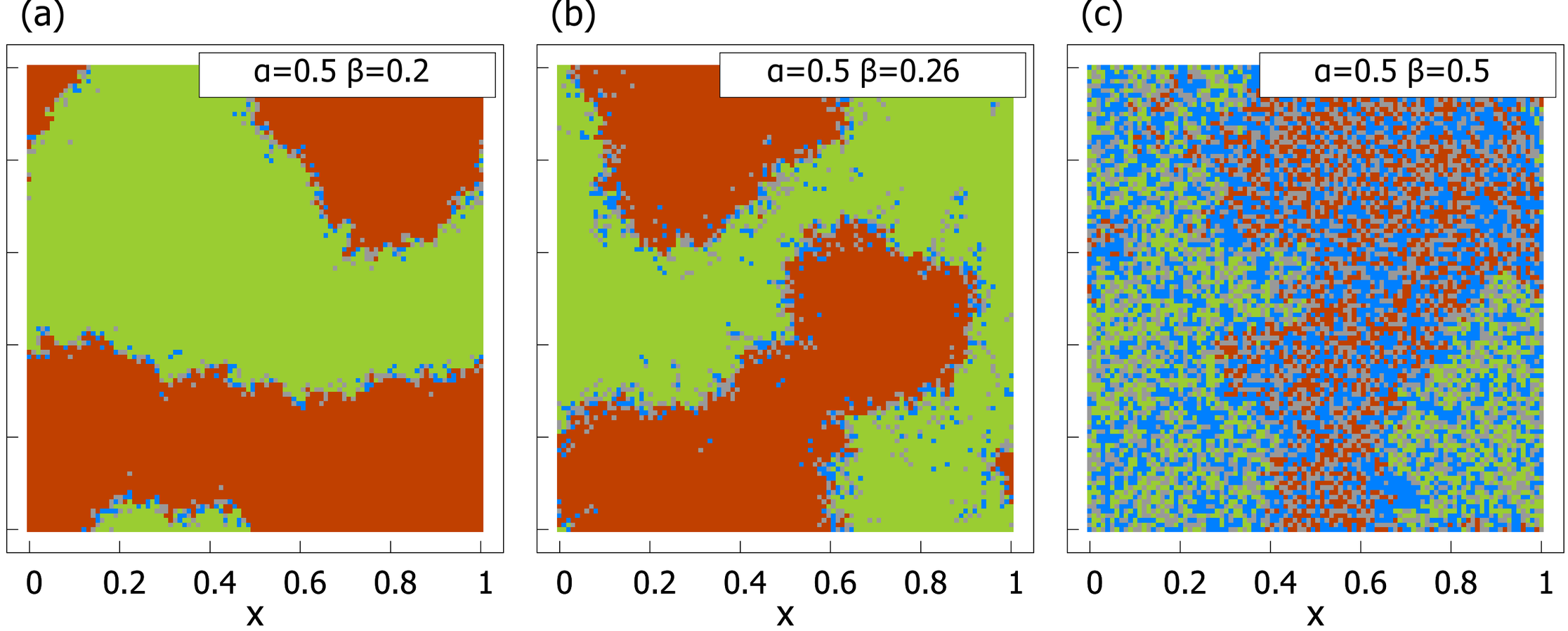

Chaos

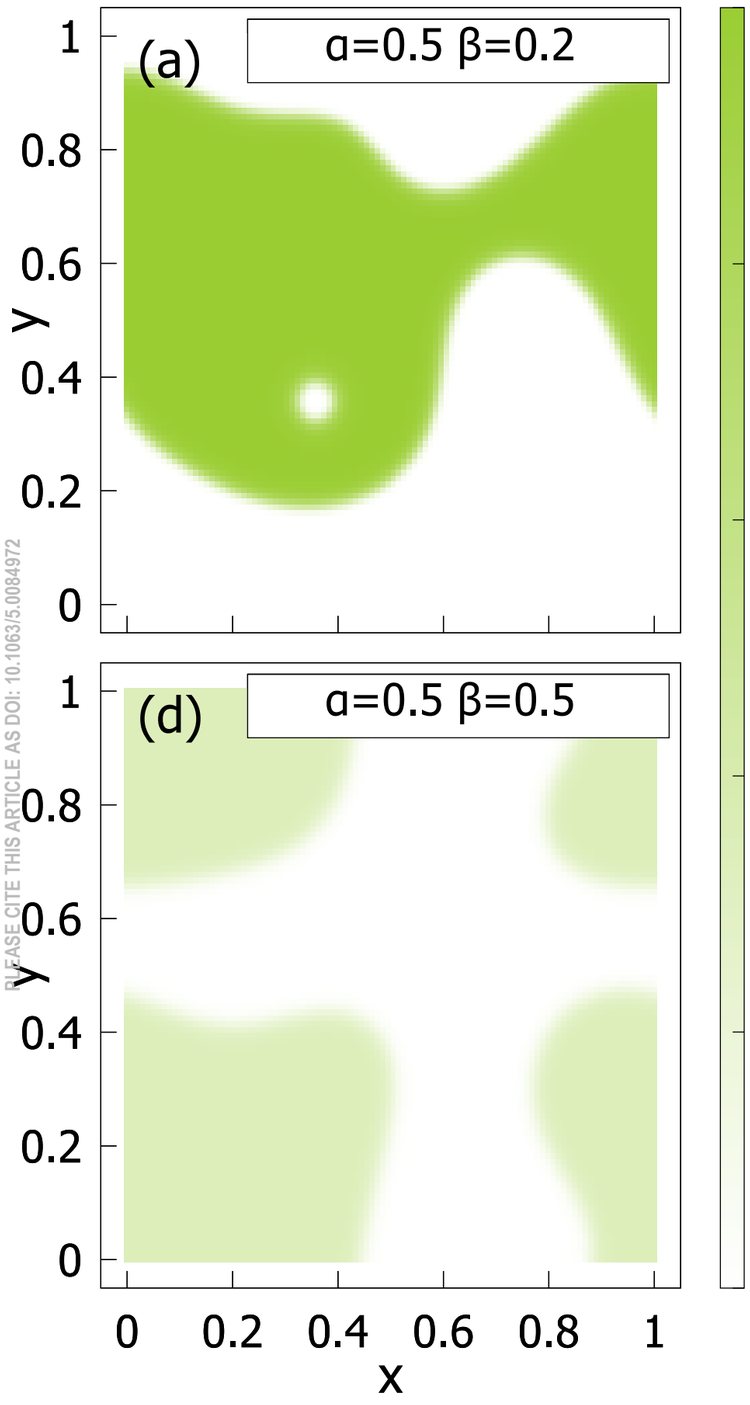

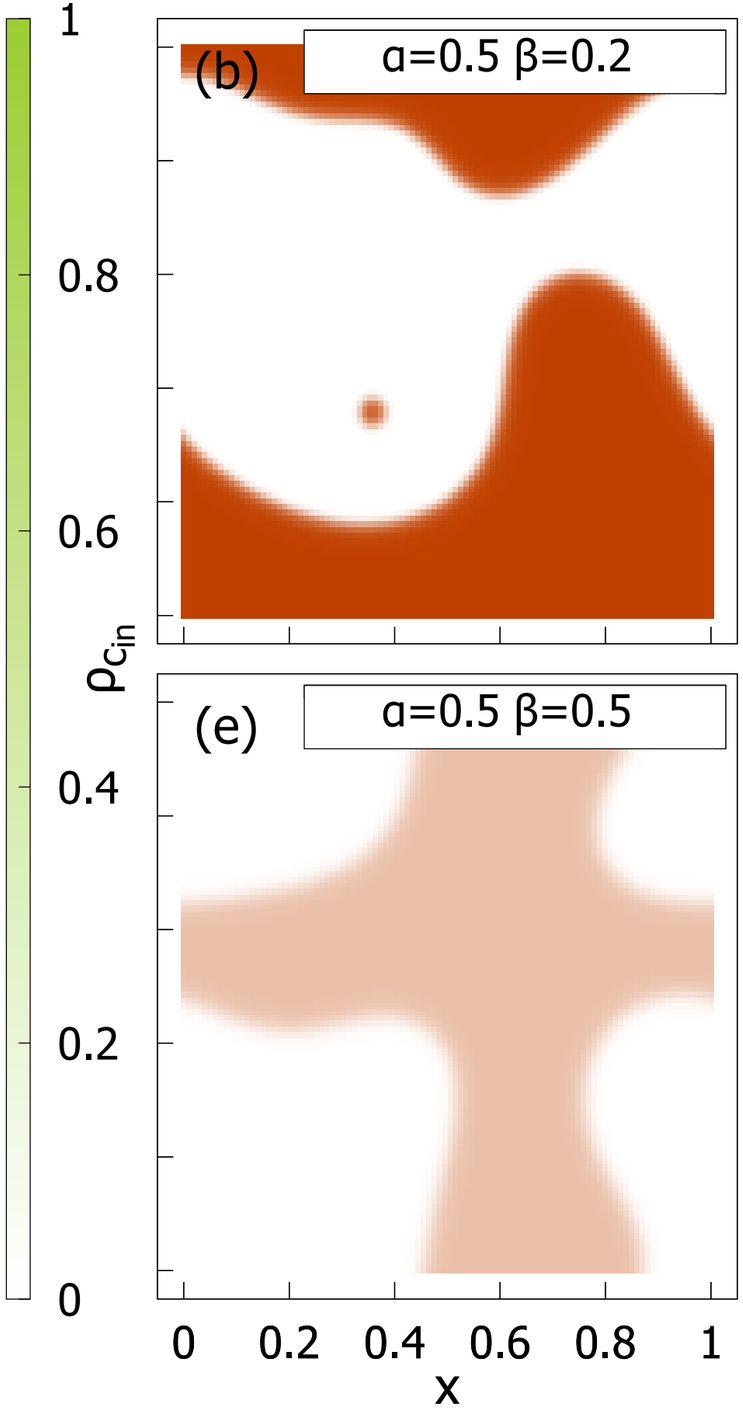

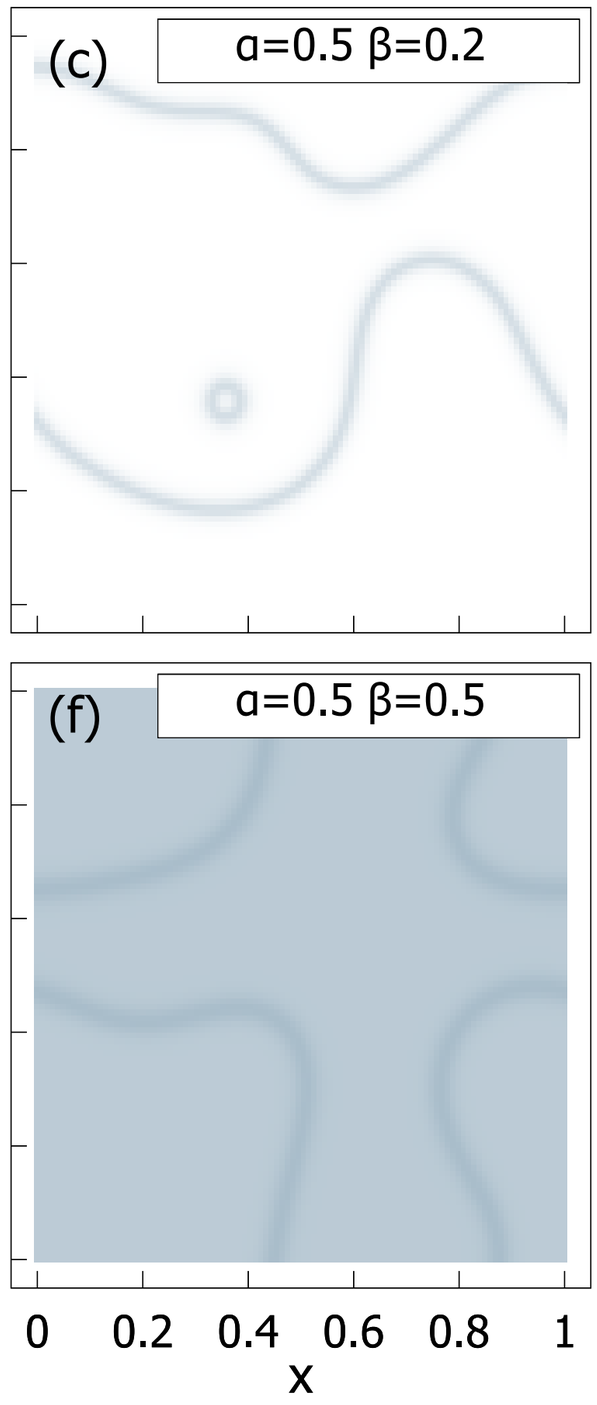

Chaos

AIP Publishing

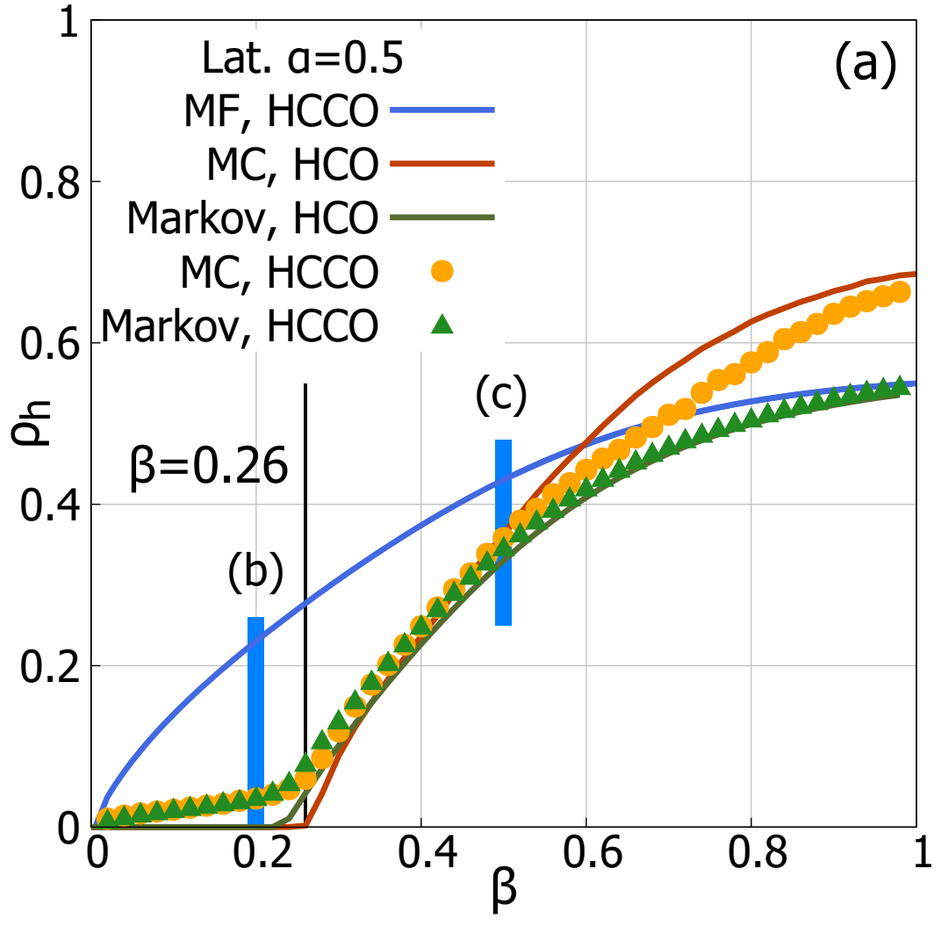

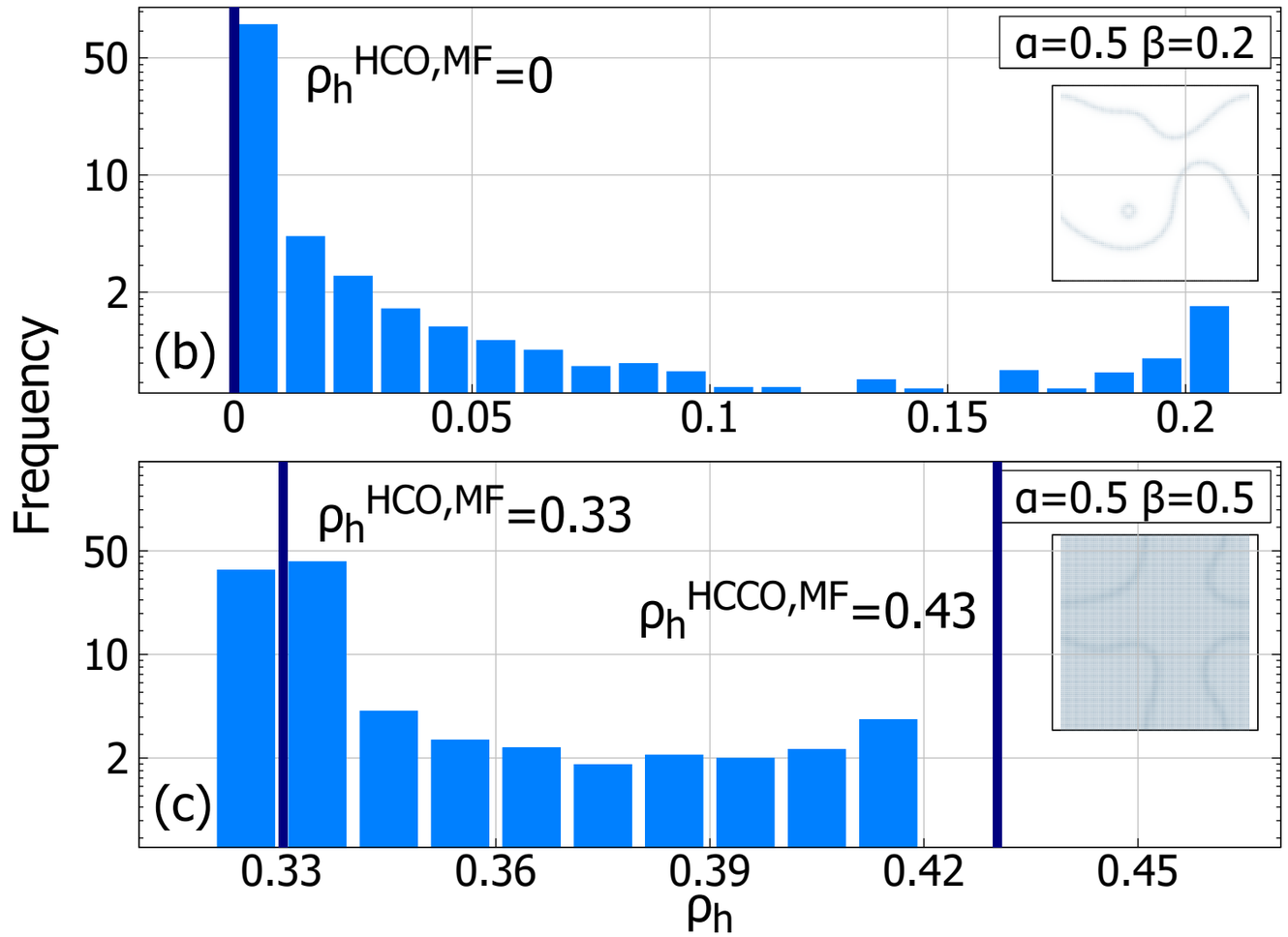

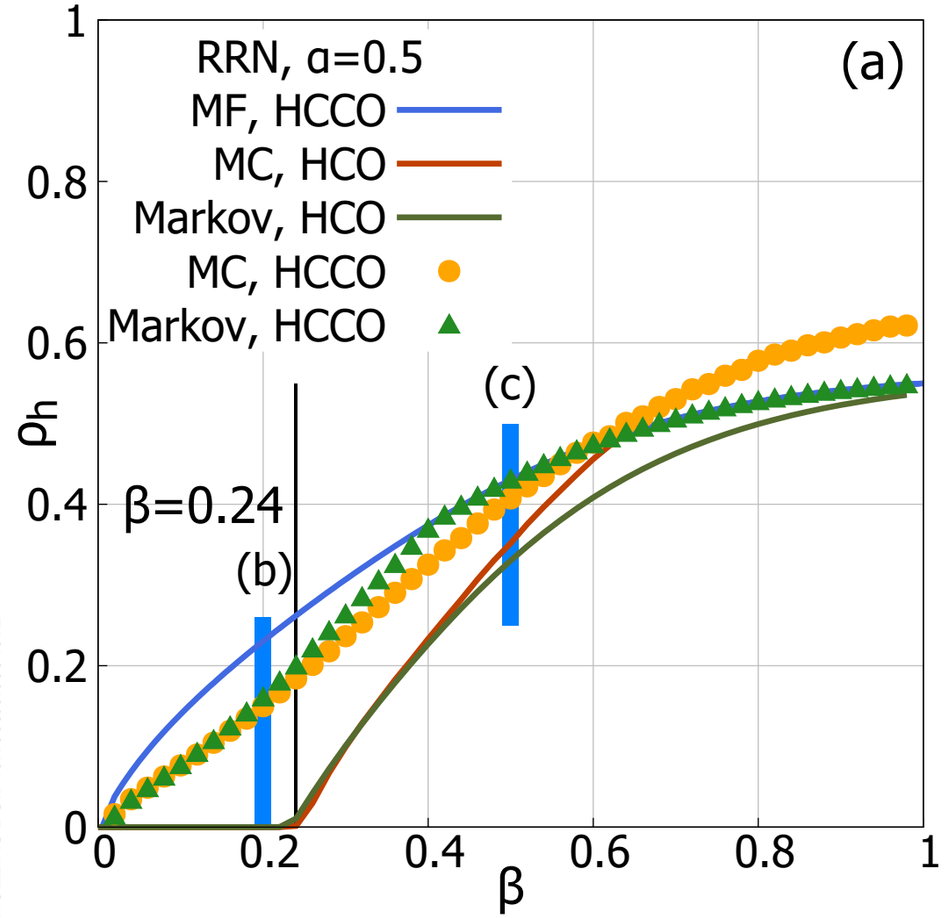

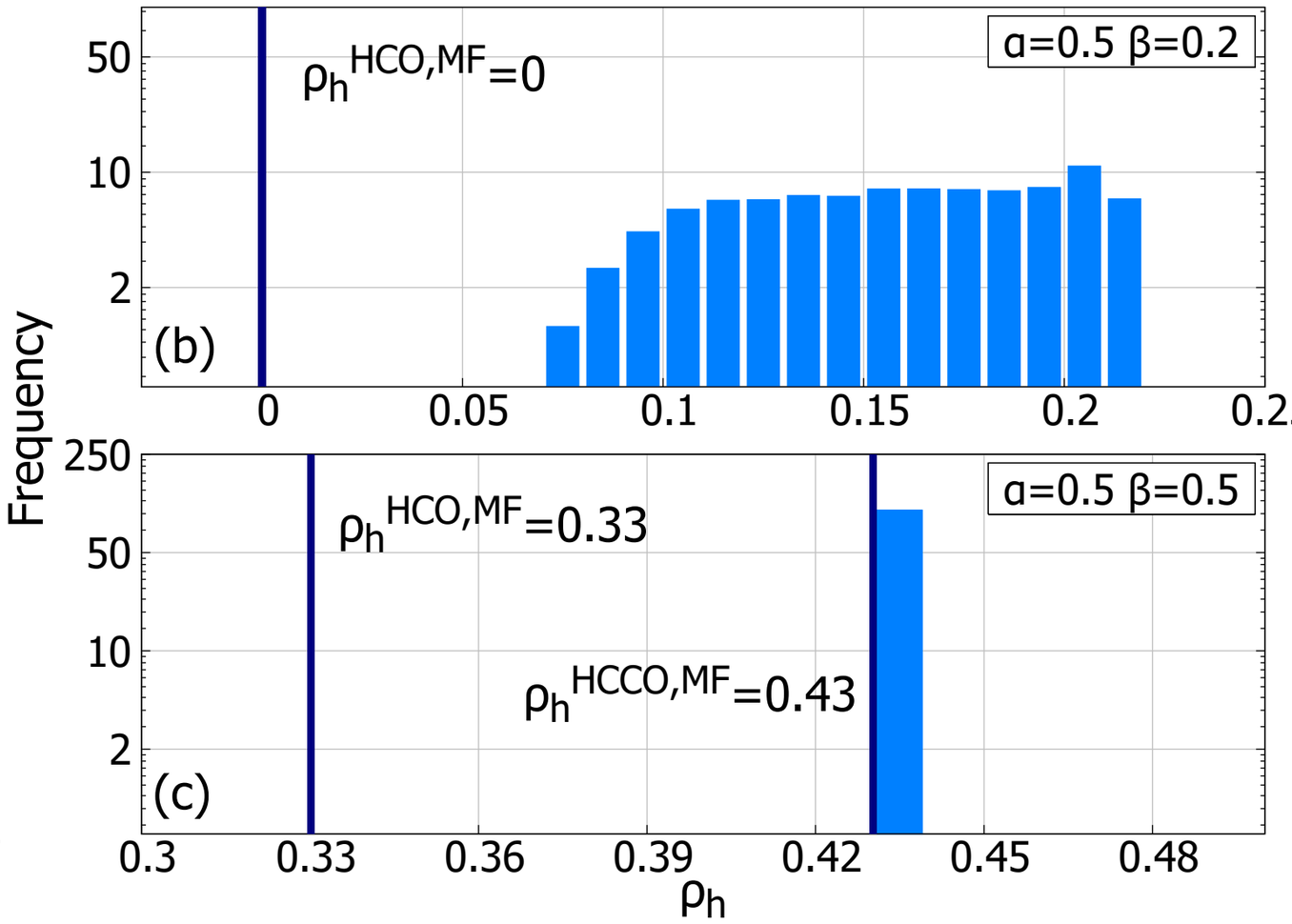

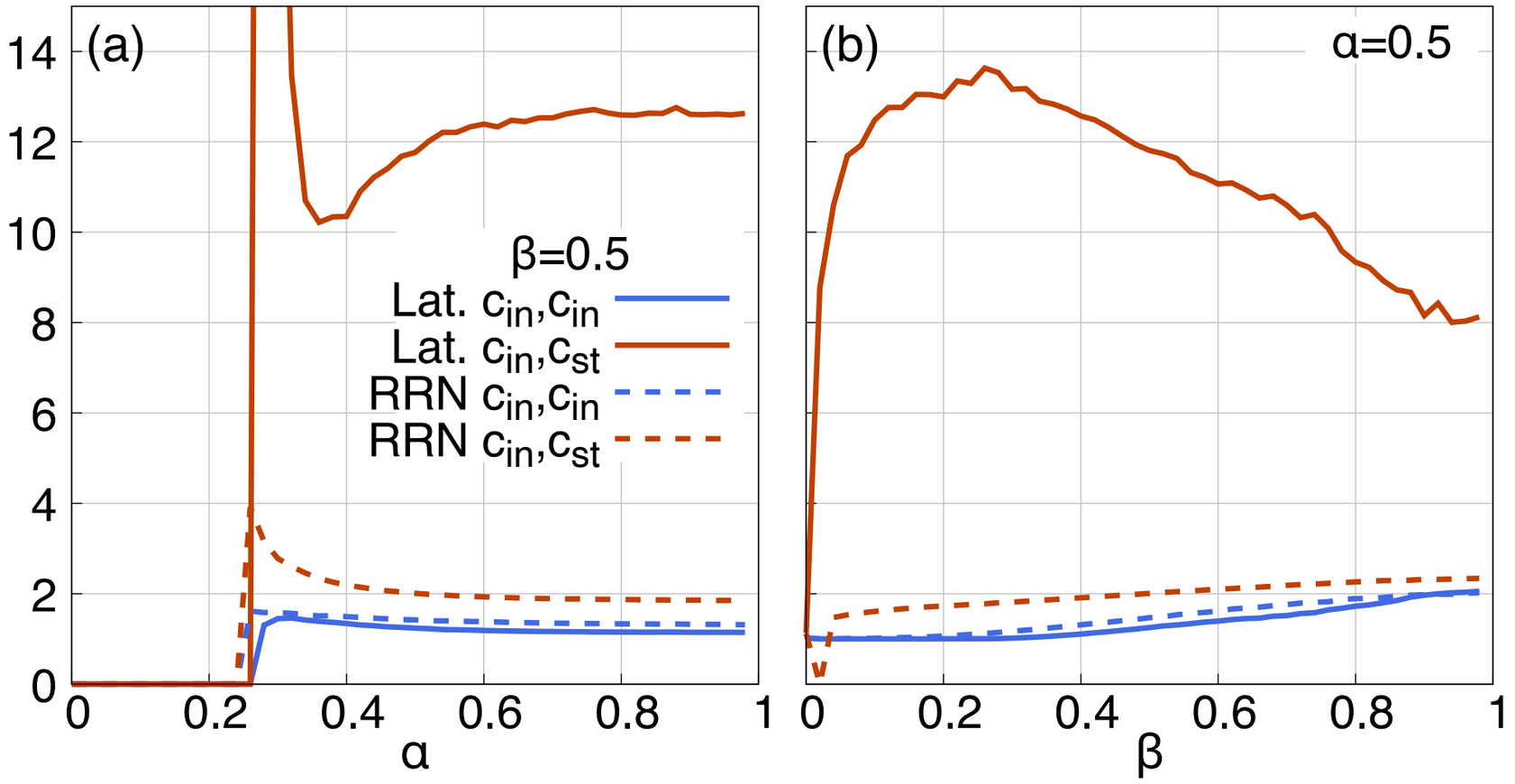

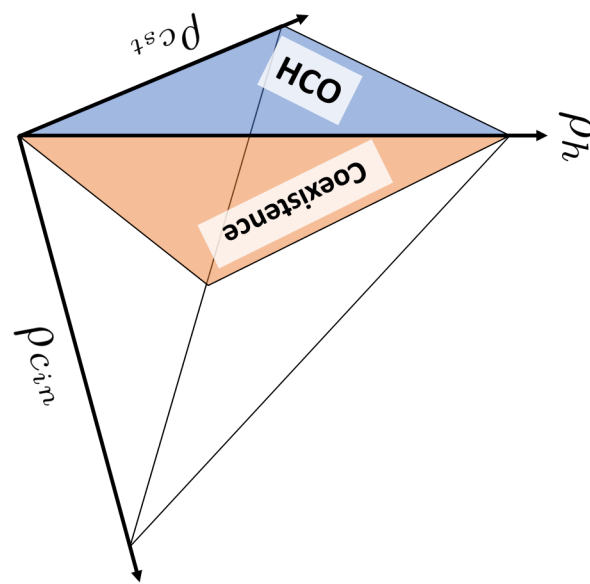

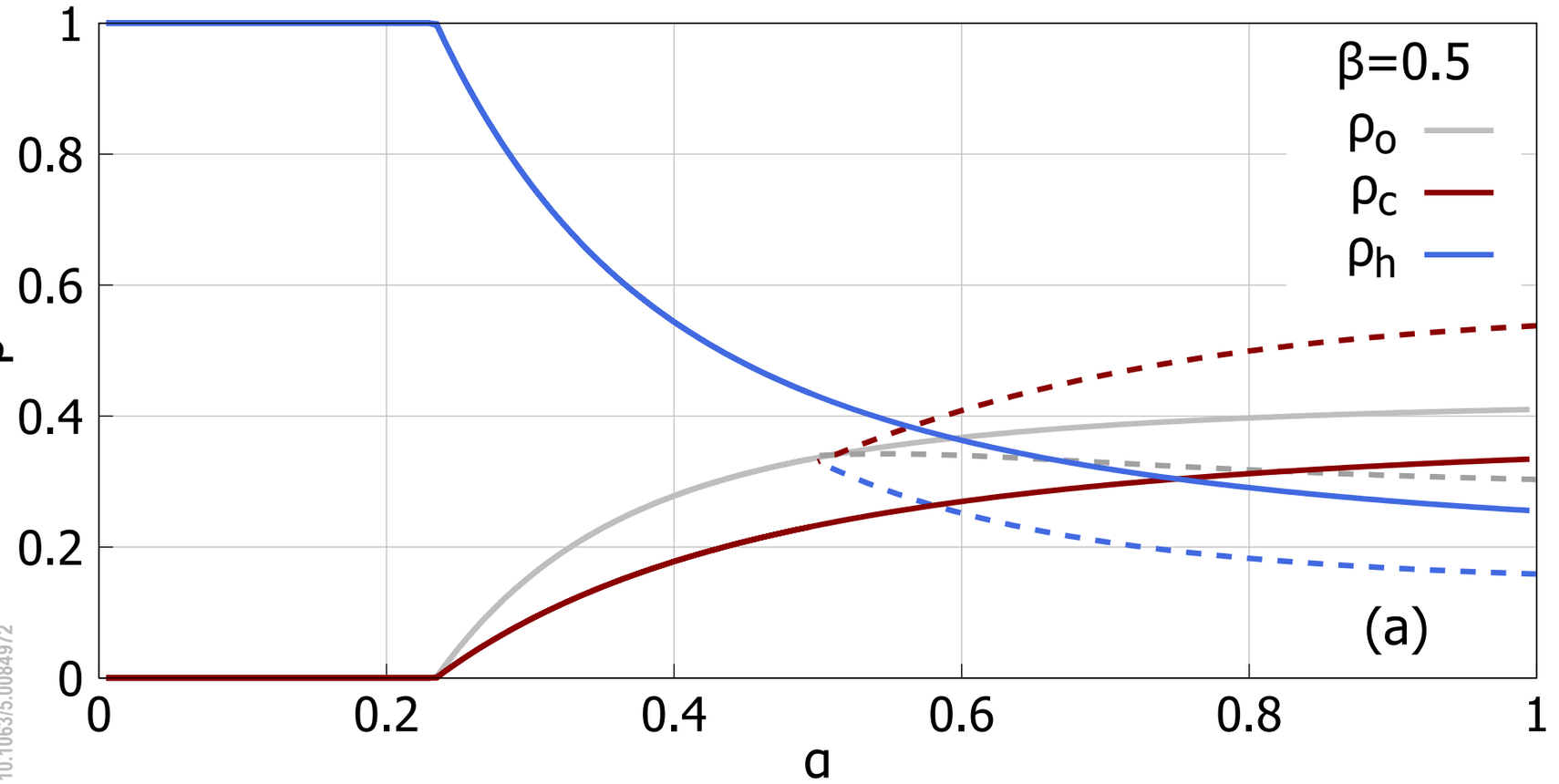

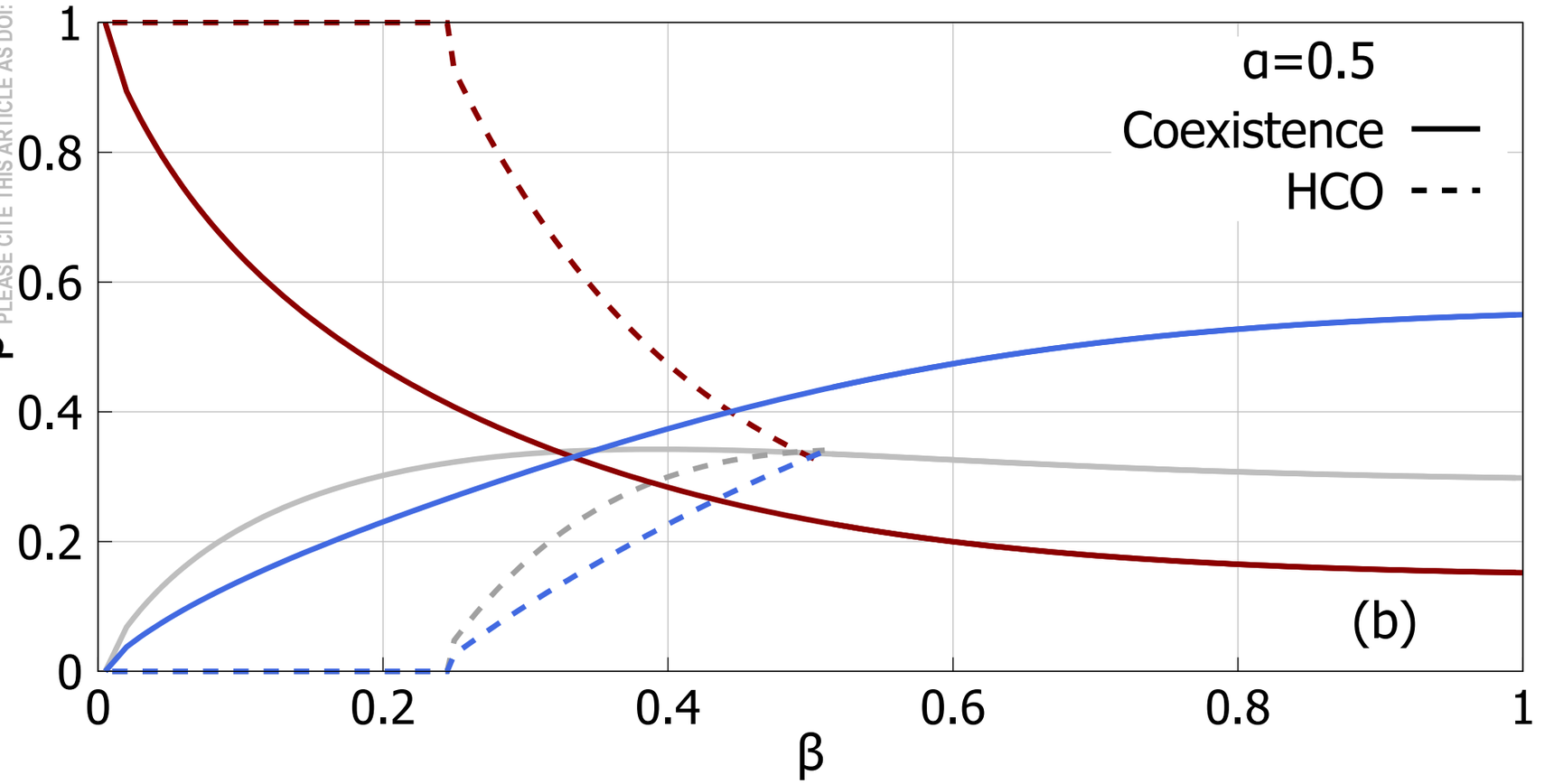

Chaos